NTIA Report 86-200

Quantifying the Effects of Terrain for VHF and Higher Frequency Application

H.T. Dougherty
E.J. Dutton

U.S. DEPARTMENT OF COMMERCE
Malcolm Baldrige, Secretary
Alfred C. Sikes, Assistant Secretary
for Communications and Information

July 1986

TABLE OF CONTENTS

LIST OF FIGURES

QUANTIFYING THE EFFECTS OF TERRAIN FOR VHF AND HIGHER FREQUENCY APPLICATION

H. T. Dougherty* and E. J. Dutton**

This report is tutorial in presentation, with emphasis on the application of engineering formulations of the effects of terrain upon terrestrial microwave systems. Many of these formulas have been available for a decade and longer, but they have not been widely used. Although they are well based in theory and experiment, their applications had been considered too detailed and tedious until the present widespread availability of personal computers. Therefore, these formulas have been presented here in a form readily adaptable as computer programs and subprograms. The units are carefully specified for use with terrain data bases for incorporation in a system design that would permit tradeoffs between terrain geometry, hardware parameters, and system performance criteria. There are additional formulations similarly well based in theory and experiment; they are not presented here, but they are adequately referenced. The readers should consider them for an increased sophistication of their system design.

The first part of the report discusses the basic geometry of great-circle-plane terrain characteristics and the application of appropriate geometrical techniques to determine if a path is line-of-sight (LOS), obstructed by a common (single) obstacle, or by separate transmitter and receiver horizons. The concept of Fresnel zones and Fresnel ellipses is introduced, and the importance of their use in determining whether a path is LOS or diffracted is discussed.

The next part of the report discusses LOS paths, and the significance of reflected signals into the direct radio path is examined. Specular reflection from finite reflecting surfaces is discussed primarily with attention directed to the theoretical reflection coefficient for smooth, infinite, planar surfaces and the consequent modifications for Earth curvature, finite surface extent, and roughness of the surface.

Then the report discusses diffraction paths with primary reliance on theory, as modified for CCIR purposes, first for isolated terrain obstacles (rounded) and then for irregular terrain, which can block both terminals on a great-circle-plane radio path. Effects of vegetation along a terrestrial-link path are also briefly considered.

Key words: clearance; diffraction; Earth's surface; engineering formulation; Fresnel zones; link design; radio horizons; reflection; terrain; terrestrial-link propagation

---

*The author is with the Colorado Radio Research Company, Westminster, CO.

**The author is with the Institute for Telecommunication Sciences, National Telecommunications and Information Administration, U.S. Department of Commerce, Boulder, CO 80303.

1. INTRODUCTION

When a telecommunications system has all or a portion of its propagation path in the vicinity of the Earth's surface, the terrain (land or sea) can introduce the propagation mechanisms of reflection, diffraction, attenuation, and scattering. These terrain effects can drastically modify the system's received signal behavior.

Terrain effects can be advantageous. For example, terrain can shield a system's terminal. That is, the likelihood of interference to or from another cochannel or adjacent-channel system can be substantially reduced by the diffraction losses caused by the intervening terrain. This can often be achieved by site selection and the positioning of the terminal's antenna.

Terrain effects can also be disadvantageous. For example, unless the likelihood of significant reflection and scattering from terrain is avoided, a system's received signal can vary sufficiently in amplitude and phase to seriously degrade the system's performance. Remedial procedures may then be required. These can often be achieved by site selection and antenna positioning or antenna design and signal processing.

Of course, site selection and antenna positioning must also accommodate such factors as: physical access to the site, the availability of power, land rental or purchase considerations, cost limitations, etc. The system engineer must then consider tradeoffs among these factors in exploiting the advantages or avoiding the disadvantages of terrain effects. To do this properly, the engineer requires quantitative estimates of terrain effects that go beyond those classical treatments of reflection and diffraction that were encountered in his or her formal training. For example, the diffraction or reflection of electromagnetic waves by terrain is usually not adequately approximated by the theory for plane-wave incidence upon an infinite or semi-infinite plane surface. For terrain applications, further modification has been required, based upon the experience of system designers and propagation researchers. These modifications are described in this report as engineering expressions and procedures that quantify the terrain effects.

2. PROPAGATION PATH INTRUSIONS

The most basic parameter for determining terrain effects is a measure of the intrusion of the terrain upon the propagation path (the wave trajectory)

from transmitter to receiver. This measure is given by the terrain obstruction heights, h_o, illustrated in Figure 1.

For the coordinates (x,y) in Figure 1, the arc $y_o(x)$ represents a reference terrain elevation, mean sea level (MSL), or any other convenient elevation. The H(x) is the terrain profile plotted in terms of its elevations above the reference elevation. The propagation path is closely approximated by the parabolic wave trajectory given by (Millington, 1957; Dougherty, 1981)

$$H_o(k,x) = H_1 + \frac{x}{d}\,(H_2 - H_1) - \frac{x(d - x)}{12.75\ k} \qquad (1a)$$

$$= H_1 + x \tan 10^{-3}\,\alpha_o + \frac{x^2}{12.75\ k}\ . \qquad (1b)$$

Here,

$H_o(k,x)$ is the trajectory elevation (m) relative to some convenient reference elevation $y_o(x)$;

H_1, H_2 are the terminal antenna elevations (m), $H_2 > H_1$;

d is the distance (km) between terminals;

x is an arbitrary distance (km) from H_1;

$\alpha_o(x)$ is the directional angle in <u>milliradians</u>, a distance x along the wave trajectory and relative to the local tangent of $y_o(x)$;

α_o is the initial directional angle (mrad) at x = 0;

12.75 is the factor 2a x 10^{-3} for an earth radius a = 6375 km; and

k is the effective Earth's radius factor (Bean and Dutton, 1968).

By differentiating (1b), we obtain the directional angle of the trajectory as

$$\tan 10^{-3}\,\alpha_o(x) = \tan 10^{-3}\,\alpha_o + \frac{x}{6.375k}\ , \qquad (1c)$$

where

$$\tan 10^{-3}\,\alpha_o(x = 0) = \tan 10^{-3}\,\alpha_o = \frac{H_2 - H_1}{d} - \frac{d}{12.75k}\ . \qquad (1d)$$

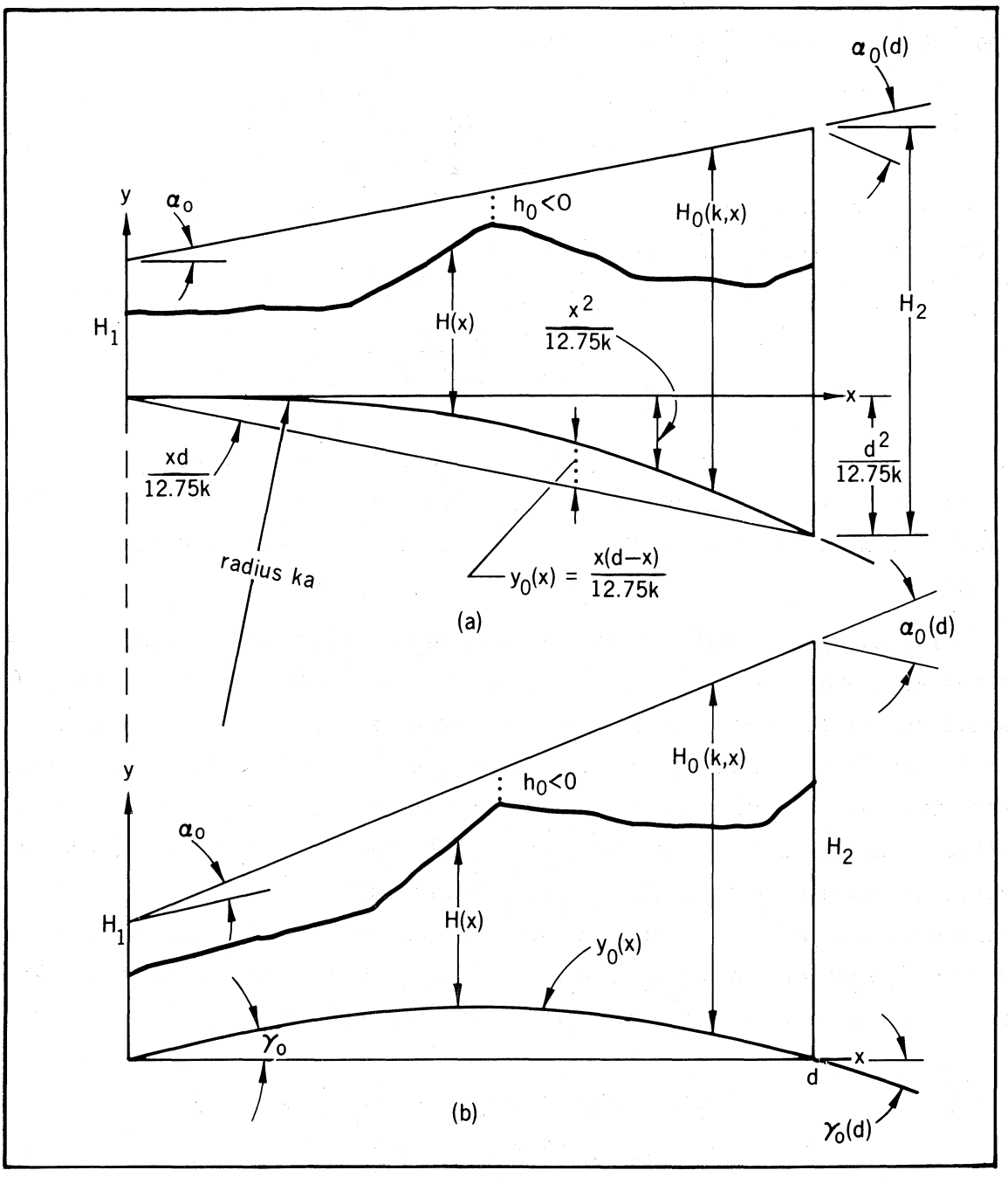

Figure 1. Great circle terrain profile geometry.

The reference terrain elevation is given by

$$y_o(x) = \frac{x(d - x)}{12.75k} \tag{1e}$$

with a local tangent, or horizontal, of

$$\gamma_o(x) = \frac{d - 2x}{12.75k} \quad . \tag{1f}$$

Here, again, the $y_o(x)$ is in meters, and $\gamma_o(x)$ is in milliradians when the distances x and d are in kilometers. At midpath, $y_o(x = d/2) = d^2/51k$, from (1d), which sets the vertical scale factor in any profile plot, as in Figure 1.

For example, a path d = 25 km will have a reference elevation curve that rises at midpath by 9.2 m for k = 4/3. If this midpath rise were plotted with equal scales for the vertical and horizontal axis, it would not be noticeably different from a straight line. Therefore, terrain profiles and radio-wave trajectories are normally plotted with markedly disparate vertical and horizontal scales; i.e., the horizontal scale is in kilometers for a vertical scale in meters. For such disparate scale factors, any normal to the curved reference elevation will plot as a vertical line, and distances along a curvilinear surface must be measured along its projection upon a Cartesian axis. Directional angles are closely approximated by their tangent

$$\alpha_o(x) = 10^3 \tan 10^{-3}\, \alpha_o(x) \text{ mrad} \quad , \tag{1g}$$

$$\gamma_o(x) = 10^3 \tan 10^{-3}\, \gamma_o(x) \text{ mrad} \quad . \tag{1h}$$

The angles are quantified by their equations and are not measureable by protractor.

To convert the expression H(k,x) from one in terms of elevations to one plotted relative to the Cartesian x axis, we add (1a) or (1b) to (1e) to obtain

$$y_o(k,x) = H_o(k,x) + \frac{x(d - x)}{12.75k} \quad . \tag{1i}$$

If the indicated k's are all the same,

$$y_o(k,x) = H_1 + \frac{x}{d}(H_2 - H_1) \quad , \tag{1j}$$

with initial slope

$$\alpha_o + \gamma_o(x = 0) = \frac{H_2 - H_1}{d} \quad . \tag{1k}$$

In Figure 1, the refractive effect of the atmosphere has been included in the value of k and the plot of $y_o(x)$, so that the reference wave trajectory plots as a straight line. Figure 1 illustrates (1b) through (1i).

Figures 2(a) and 2(b) depict line-of-sight situations where the wave trajectory elevations exceed those of the terrain. The closest approach of the $H_o(k,x)$ to the terrain $H(x)$ determines the maximum intrusion of the terrain upon the trajectory; this minimum vertical interval is a negative obstacle height, $h_o < 0$. For the maximum intrusion without obstruction, the grazing condition is $H_o(k,x) = H(x)$; then $h_o = 0$. In Figure 2(c), the terrain actually obstructs the reference trajectory so that the obstacle is positive, $h_o > 0$. The peak terrain elevation at P also constitutes the horizon common to both terminals.

In Figure 2(d), the horizons, at P_1 and P_2, permit determination of the obstacle height, $h_o > 0$. The trajectories have been extended from their terminals to beyond their horizons; their intersection at P determines an equivalent obstructive terrain peak and the obstacle height, $h_o > 0$ (Dougherty, 1968). The expressions for the wave trajectory to each horizon are readily written. For the trajectory from H_1, we determine $H_1(k,x)$ by substituting x_1 and $H(x_1)$ for d and H_2 in (1d) and subtracting the $y_o(x)$ given by (1f) to obtain

$$H_1(k,x) = H_1 + x \tan 10^{-3}\,\alpha_1 + \frac{x_1^2}{12.75k} \quad , \tag{2a}$$

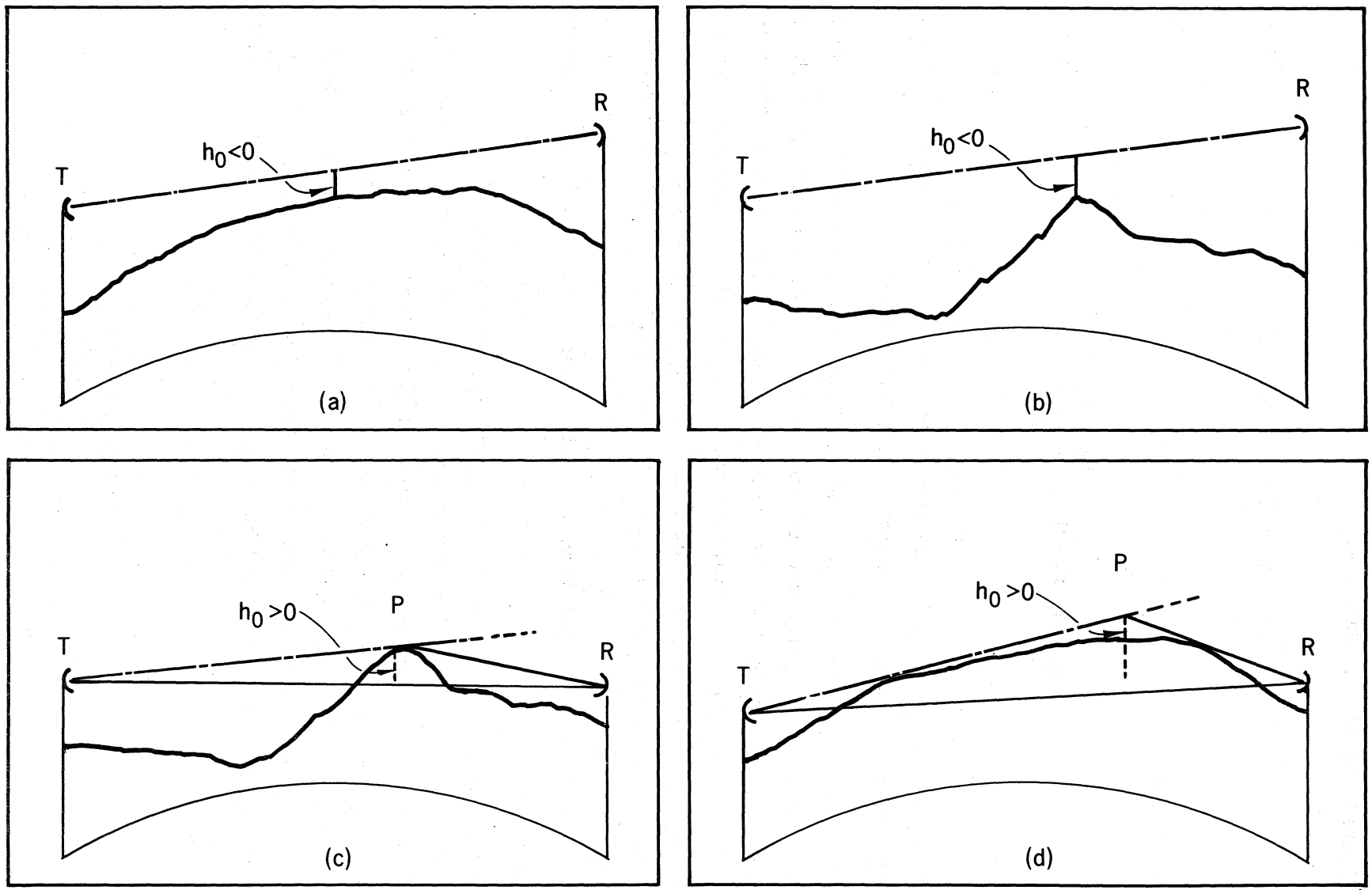

Figure 2. Various terrain obstacle heights and their intrusion into the propagation path.

$$\alpha_1(x) = \frac{H(x_1) - H_1}{x_1} - \frac{x_1}{12.75k} \quad . \tag{2b}$$

Differentiating (2a),

$$\alpha_1(x) = \alpha_1 + \frac{x}{6.375k} \quad , \tag{2c}$$

where $H(x_1)$ is the horizon elevation at $x = x_1$. Similarly, for the trajectory from P_2 to H_2, by derivation with aid of Figure 1, one obtains

$$H_2(k,x) = H(x_2) + (x - x_2) \tan 10^{-3} a_2 + \frac{(x - x_2)^2}{12.75k} \quad , \tag{3a}$$

$$\tan 10^{-3} a_2 = \frac{H_2 - H(x_2)}{d - x_2} - \frac{d - x_2}{12.75k} \quad , \tag{3b}$$

$$\alpha_2(x) = \alpha_2 + \frac{(x - x_2)}{6.375k} \quad , \tag{3c}$$

where $H(x_2)$ is the horizon elevation at $x = x_2$.

2.1 Fresnel Zones

To determine their effect upon the radio wave, we can express the terrain obstacle heights in terms of Fresnel zone radii. Consider Figure 3, where a transmitting source at T radiates energy in a spherical wave front to a receiving antenna at R. There is a first Fresnel zone centered at P on the wave front of the propagation path TR. The radius of this zone is given by

$$F_1 = 548 \sqrt{\frac{d_1 d_2}{fd}} \quad . \tag{4a}$$

Here the F_1 is given in meters when the distances d_1, d_2, and d are in kilometers and the frequency f is in megahertz. For this choice of units, the 548

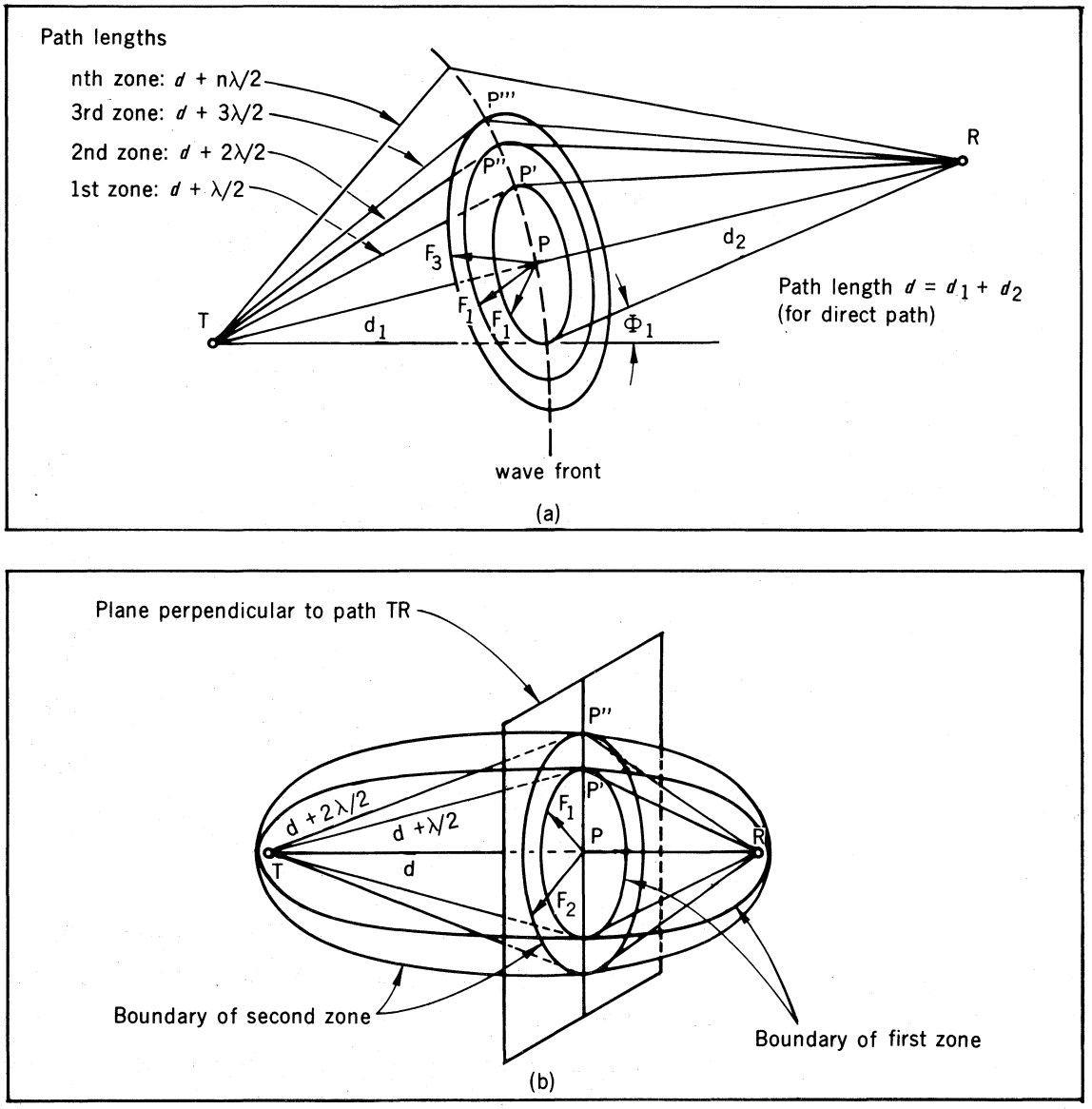

Figure 3. Cross-section of a radio path showing Fresnel zones and Fresnel ellipsoids.

in (2a) results from taking the square root of the speed of light in kilometers per second. The boundary of this first Fresnel zone is the locus of all points P' for which the path TP'R exceeds that of TPR by one-half wavelength, $\lambda/2$. By extension, the boundary of the nth zone (an annular ring for $n > 1.0$) is given by the locus of all points $P^{(n)}$ such that $TP^{(n)}R$ - TPR is $n\lambda/2$. The radius to the boundary of the nth zone is given by

$$F_n = \sqrt{n}\ F_1 \quad . \tag{4b}$$

In addition to the Fresnel zone radii, we can also define a Fresnel-zone angle Φ_1, shown in Figure 3(a) and given by

$$\sin \Phi_1 = \frac{F_1 d}{d_1 d_2} \quad . \tag{4c}$$

This angle may be approximated directly by

$$\Phi_1 \approx \frac{F_1 d}{d_1 d_2} \tag{4d}$$

in milliradians, when F_1 is in meters and the distances are in kilometers. In general,

$$\sin \Phi_n = \sqrt{n}\ \sin\Phi_1 \quad . \tag{4e}$$

When we consider all possible wave fronts between T and R, the locus of P' defines a first Fresnel ellipsoid in space, as illustrated in Figure 3(b). Figure 3(b) also depicts the second Fresnel ellipsoid. There are similar higher-order Fresnel ellipsoids, all having the common pair of focii, at T and R, a distance d apart. If the closest approach of the terrain from below just touched the outer (second) ellipsoid of Figure 3(b), we would say the propagation path had a second-zone (n = 2) clearance and $h_o = -F_2 < 0$. For Figures 2(a) and 2(b), the Fresnel-zonal clearances would be given by

$$\sqrt{n} = |h_o/F_1| \quad . \tag{5}$$

The F_1 are given by (4a). If the TR line in Figure 3(b) were a reference trajectory obstructed by a single terrain feature that peaked at P", the obstacle height would be $h_o = F_2 > 0$.

When used as a measure of displacement, the n in (4b) through (5) is not necessarily an integer. An example is given in Section 2.4 of this report.

2.2 Modes of LOS Propagation

Figures 2(a) and 2(b) illustrate line-of-sight (LOS) paths. The radio wave energy travels from transmitting terminal T to receiving terminal R, primarily by the direct space-wave path that is indicated by the straight line. However, the emitted radio wave is also incident upon the terrain visible from T. Portions of this incident wave would be reflected by the terrain, possibly toward the receiving terminal. The incident wave will also produce a ground wave traveling along the terrain toward the receiving terminal.

If the terrain obstacle height is sufficiently negative, the terrain effect can be adequately represented by reflection theory. Then, the total field E may be expressed, relative to the free-space field E_0, by adding the reflected components to the direct wave component

$$E/E_0 = a(R) = g - \sum_i g_i R_i e^{-j\phi_i} \quad . \tag{6}$$

Here the g and g_i are the combined effects of the transmitting and receiving antenna gain patterns for, respectively, the direct and each of the reflected propagation path trajectories. The R_i are the effective reflection coefficients, and the ϕ_i are the relative phase lags of these reflected-wave propagation paths. See Section 3.

If the LOS terrain obstacle heights are not sufficiently negative, it is more efficient to describe their effects by diffraction theory. Then the total field E, relative to the free-space field E_0, is expressed as a diffraction function for negative obstacle heights,

$$E/E_0 = a(h_o < 0), \text{ for } n \leq n_c \quad . \tag{7}$$

See Section 4.

Any value of n that would serve as a criterion n_c in choosing between the application of the reflection theory in (6) and that of the diffraction theory in (7) must be somewhat arbitrary. Reflection theory could be used for an n = 1.0, but it would become increasingly inappropriate as n approached zero. For convenience, we have chosen the criterion as $n_c = 0.3$. That is, when the Fresnel-zone clearance is greater than $n_c = 0.3$, equation (6) is appropriate. Otherwise, equation (7) is preferred. Note that this clearance criterion corresponds to a fraction $\sqrt{n_c} \approx 0.55$ of the first Fresnel-radius F_1, sometimes approximated as $0.6F_1$. At the clearance corresponding to n = 0.3, the long-term total field is equal to the free-space field, $a(h < 0) = 1.0$.

2.3 Determining the LOS Obstacle Height

The minimum path clearance is a function of the terrain elevations, the terminal elevations, and the effective Earth radius. A common procedure is to plot the terrain profile for a k = 4/3 Earth and determine the minimum terrain/trajectory height interval h(k,x') graphically as in Figure 2. However, this minimum interval can also be computed. For example, this height interval in Figure 4, for an effective-Earth-radius factor k and at a distance x from one terminal of an LOS path, is

$$h(k,x) = H(x) - H_o(k,x) \quad , \tag{8}$$

where $H_o(k,x)$ is given by (1a) or (1b), and H(x) is the elevation of the terrain in meters at the distance x. The value of x = x', which minimizes h(k,x), determines the Fresnel-zone clearance

$$\sqrt{n} = |h(k,x')/F_1| \quad , \tag{9}$$

where F_1 is determined from (4a) with d_1 and d_2 replaced by x' and d-x'. An example is given in Section 2.6. The minimum, h(k,x'), is often most readily obtained by computer algorithmic procedures using a terrain data base.

2.4 Modes of Transhorizon Propagation

Figures 2(c) and 2(d) depict transhorizon paths for which the field is best described by both diffraction theory and tropospheric scatter theory. For small positive obstacle heights, the diffraction field given by

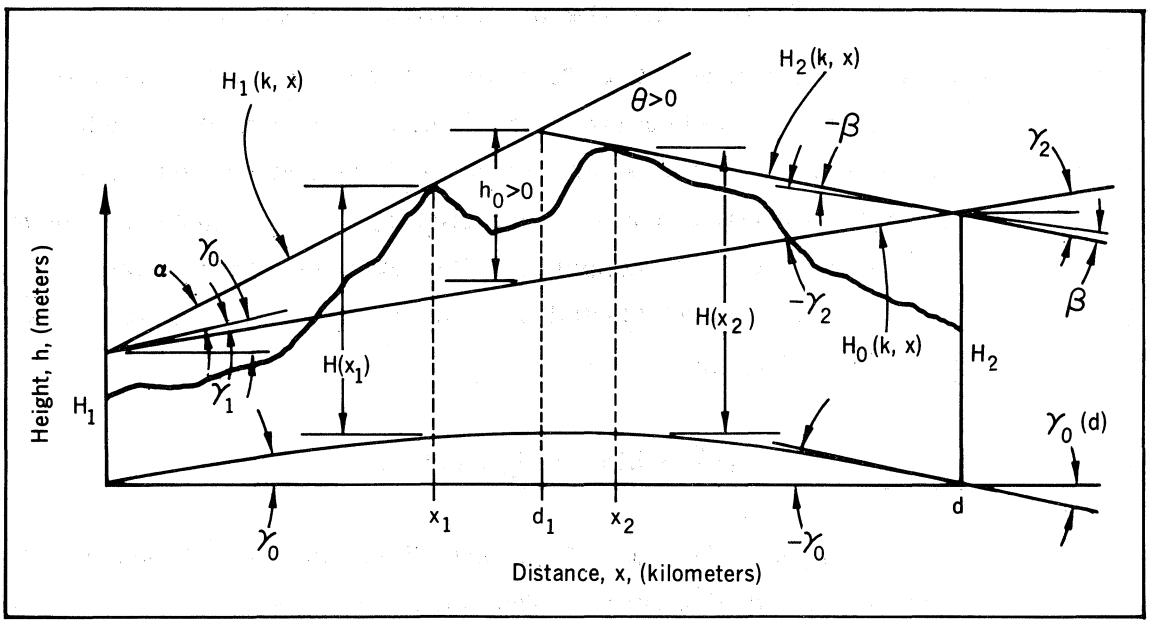

Figure 4. Transhorizon radio path directional angle geometry.

$$E/E_0 = a(h_o > 0) \tag{10}$$

will predominate. Here, we have assumed only a direct path, as illustrated in Figures 2(c) and 2(d). However, there can be additional propagation paths. This is because transhorizon paths contain two LOS sections, one between each terminal and its horizon. This will permit additional paths involving reflection and scatter to occur.

For more positive obstacle heights [$h_o > 0$ and $n > 0.3$ in (9)], the tropospheric scatter plays an increasingly important role. Its contribution must then be determined and added vectorially to the diffracted field (CCIR, 1986a; Rice et al., 1967).

2.5 The Transhorizon Clearance

For a transhorizon path such as in Figure 4, the horizons are most readily determined from a terrain profile for an effective-Earth-radius-factor k. We can designate the terrain elevations at the horizons as $H(x_1)$ and $H(x_2)$ in meters, where x_1 and $d - x_2$ are the respective distances from each terminal to its horizon. Then, for the angles indicated in Figure 4, we note that*

$$\theta = \alpha - \gamma_1 - [\beta - \gamma_2] = \alpha - \beta + \frac{2d}{12.75k} , \tag{11a}$$

where

$$\alpha \approx 10^3 \tan 10^{-3}\, \alpha = \frac{H(x_1) - H_1}{x_1} - \frac{x_1}{12.75k} \tag{11b}$$

and

$$-\beta \approx 10^3 \tan 10^{-3}\, \beta = \frac{H(x_2) - H_2}{d - x_2} - \frac{d - x_2}{12.75k} . \tag{11c}$$

*Note γ_1 is negative and β is negative relative to the local endpoint tangents in Figure 4. This fact must be taken into account when comparing (11a) and (14) with Figure 4.

Here,

θ = the diffraction angle in milliradians,

H_1, H_2 = the terminal antenna elevations in meters,

x_1, x_2 = the distances in kilometers from H_1 to the two horizons, and

12.75 = the $2a \times 10^{-3}$ for an earth radius a = 6375 km.

Commonly, k = 4/3, and the positive obstacle height may be determined with the aid of

$$\gamma_1 \approx 10^3 \tan 10^{-3} \gamma = \frac{H_2 - H_1}{d} - \frac{d}{12.75k} \qquad (12a)$$

and

$$\gamma_2 = \gamma_1 + \frac{2d}{12.75k} \qquad (12b)$$

in milliradians. The distance d_1 in Figure 4 is approximately given by the Law of Sines (see footnote on preceding page).

$$d_1 \approx \left| \frac{d}{\theta} [\beta - \gamma_2] \right| \quad . \qquad (13)$$

The transhorizon obstruction is given by

$$\sqrt{n} = \left| \frac{d_1}{F_1} \sin 10^{-3}(\alpha - \gamma_1) \right| \times 10^3 \quad , \qquad (14)$$

where F_1 is given by (4a) with d_2 replaced by $d - d_1$. An example is given in Section 2.6.

2.6 Examples

2.6.1 An LOS Path

Consider the LOS terrain profile illustrated by Figure 5. We assume that a proper effective-Earth radius factor is k = 4/3. Therefore, terrain elevations H(x) have been plotted in Figure 5 relative to the reference elevation and slope

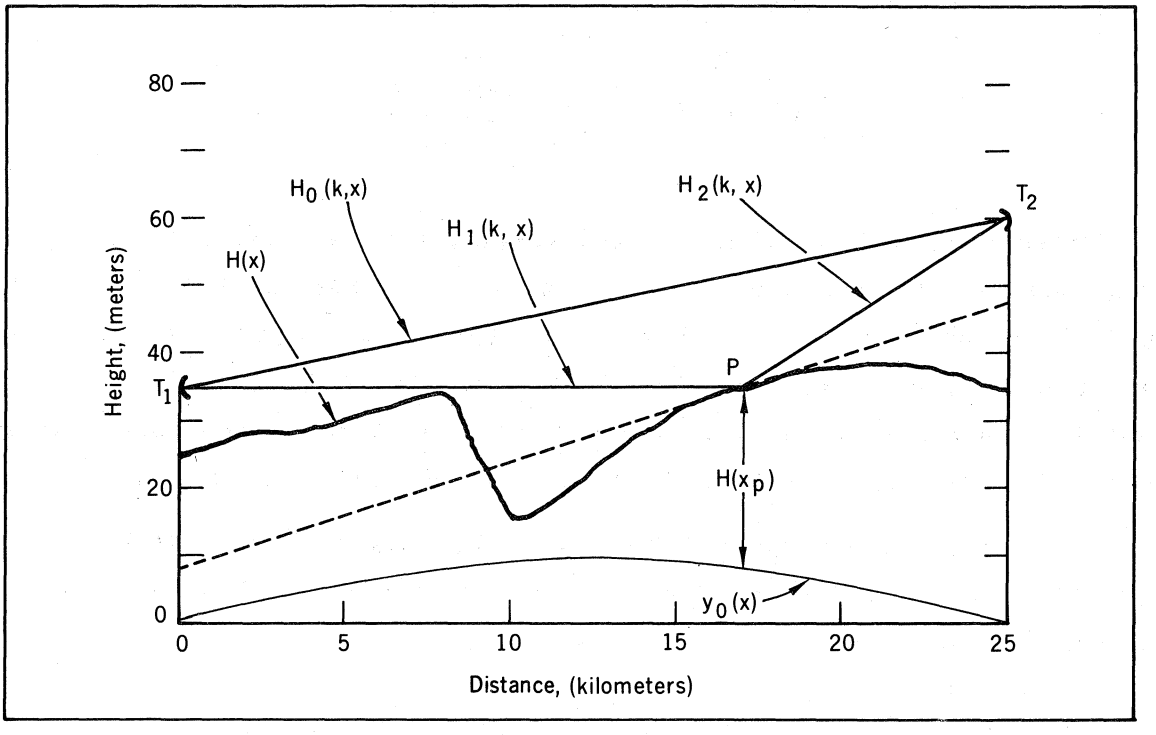

Figure 5. A terrain profile example on a line-of-sight path.

$$y_0(x) = \frac{x(25 - x)}{17} \quad , \quad \gamma_0(x) = \frac{25 - 2x}{17} \quad ,$$

from (1e) and (1f). The direct-wave path from $H_1 = 35$ m at T_1, to $H_2 = 60$ m at T_2, d = 25 km away, is also plotted. From (1j) and Figure 5, the path is clearly a straight line

$$y(k,x) = 35 + x \quad ,$$

with a slope of 1.0 mrad (rises 25 m over a distance of 25 km). The equation for the wave propagation path from (1i) is, for k = 4/3,

$$H(k,x) = 35 + x - \frac{x(25 - x)}{17} \quad ,$$

and clearly quadratic. This curved propagation path appears as a straight line when plotted relative to its effective Earth radius; i.e., (1e) and (1a) have the same value of k. If the terrain profile of Figure 5 were plotted for any other value of k, the propagation path would be curved. The initial elevation angle γ_1 from (1d) is -0.47 mrad relative to the local horizontal $\gamma_0(x = 0) = 1.47$ mrad; hence, the T_1T_2 slope of 0.001 (1.0 mrad).

At x = 8 km, the terrain elevation H(x = 8) = 26 m above the reference elevation $y_0(x = 8) = 8$ m plots as y(4/3, x = 8) = 26 + 8 = 34 m. Since the wave path at x = 8 km is

$$y(k = 4/3,\ x = 8) = 35 + 8 = 43 \text{ m} \quad ,$$

the height-interval (8)

$$h(k,x) = y(x) - y(k,x) = H(x) - H(k,x)$$

is

$$h(4/3,\ 8) = 34 - 43 = -9 \text{ m} \quad .$$

From (4a) at f = 4 GHz,

$$F_1 = 548\sqrt{\frac{8(17)}{25(4000)}} = 20.21 \text{ m}$$

and from (5)

$$\sqrt{n} = |-9/20.21| = 0.445$$

and $n = 0.198 < n_c$. Therefore, the effect of the terrain feature at $x = 8$ km should be evaluated by (7) or the diffraction theory of Section 4.

There is another local minimum clearance in Figure 5 at $x = 17$ km for which $y(17) = 35$ or $H(17) = 27$ m. For the wave path, $y(4/3, 17) = 35 + 17 = 52$, so the clearance is $H(4/3, 17) = 35 - 52 = -17$ m. Since F_1 is the same for $x = 8$ and $x = 17$,

$$\sqrt{n} = |-17/20.21| = 0.841$$

and $n = 0.707 > n_c$. The effect of this local portion of terrain is best evaluated by reflection (6) and the reflection theory of Section 3. From (4d) and (4e), the Fresnel-zone angle is

$$\Phi_n \simeq 0.841 \quad \frac{20.21(25)}{17(8)} = 3.125 \text{ mrad} \quad ,$$

or approximately 0.18 degrees.

2.6.2 A Transhorizon Path

If the terminals T_1 and T_2 of Figure 5 were lowered to T_1' and T_2' at $H_1 = 30$ m and $H_2 = 38.3$ m, the path becomes a (noncommon horizon) transhorizon path. The two horizons would then be:

$$P_1 \text{ at } y(x_1) = 34 \text{ m or } H(x_1) = 26 \text{ m at } x_1 = 8 \text{ km}$$

and

$$P_2 \text{ at } y(x_2) = 38.3 \text{ m or } H(x_2) = 33.4 \text{ m at } x_2 = 21 \text{ km} \quad .$$

From (2b), the initial elevation angle for the direct-wave path T_1' to P_1 would be

$$\alpha = \frac{26-30}{8} - \frac{8}{17} = -0.9706 \text{ mrad} \quad ,$$

relative to the initial horizontal (1f), $\gamma_0 = 1.4705$. From (11c), the final directional angle for the direct-path P_2 to T_2' would be

$$-\beta = \frac{33.4 - 38.3}{4} - \frac{4}{17} = -1.4603 \text{ mrad} \quad ,$$

relative to the local horizontal (1f), $\gamma_0(x = d) = -1.4705$.

The initial and final directional angles of the fictitious direct path T_1' to T_2' would be given by (12a) and (12b) as

$$\gamma_1 = \frac{38.3 - 30}{25} - \frac{25}{17} = -1.1386 \text{ mrad}$$

and

$$\gamma_2 = -1.1386 + \frac{50}{17} = 1.8026 \text{ mrad} \quad .$$

From (11a)

$$\theta = -0.9706 - 1.4603 + \frac{50}{17} = 0.51 \text{ mrad} \quad .$$

From (13), the extensions of T_1' and P_1 and T_2' to P_2 will intersect at

$$d_1 = \frac{25}{0.51}(0.3423) = 16.8 \quad .$$

The $y(d_1) = 38.4$ m, and the direct path T_1' T_2' rises to 35.6 m at $d_1 = 16.8$ km. From (4a) at $d_1 = 16.8$, $F_1 = 20.34$ m. The transhorizon Fresnel-zone obstruction (14) is

$$\sqrt{n} = \frac{2.8}{20.34} \quad 0.14$$

or $n \approx 0.02$.

3. REFLECTION

When the Fresnel-zone clearance of (5) exceeds $\sqrt{n_c} = 0.548$ (i.e., $n_c \approx 0.3$) over a portion of the terrain profile, the received field reflected from that portion of the terrain could be one of the contributing terms to the summation in (6). We must then establish for the direct and ith reflected path:

- g, g_i The rms antenna power-gain (voltage-gain) factors*. These are functions of the transmitting and receiving antenna gain patterns and the directions of the direct and reflected wave paths.
- ϕ_1 The relative path delay phase $2\pi\delta/\lambda$, δ = TPR - TR. The λ is the transmission wavelength.
- R_i The effective reflection coefficient. This is a function of the reflection angle, the wavelength, and the shape and roughness of the reflecting surface.

Each of these parameters is a function of the path geometry.

3.1 Reflection Path Geometry

Figure 6 illustrates the significant geometrical parameters for reflection. The H_1 and H_2 identify the elevations of the T and R terminals. The P marks the specular reflection point on the plane that is tangent to the terrain surface at P. There,

- γ_1 is the "initial" (i.e., x = 0) direction of the direct path in milliradians, relative to local horizontal plane;
- γ_2 is the "final" (i.e., x = d) direction in milliradians of the direct path, relative to local horizontal plane;
- α is the initial direction in milliradians of the reflected path, relative to local horizontal plane;
- β is the final direction in milliradians of the reflected path, relative to local horizontal plane;

---

*Note that here and in future use, the symbol g represents the ratio of two voltages so that the commonly used power gain, G, in decibels relative to isotropic is given by $G = 20 \log_{10} g$. This is in accordance with the usage in equation (6).

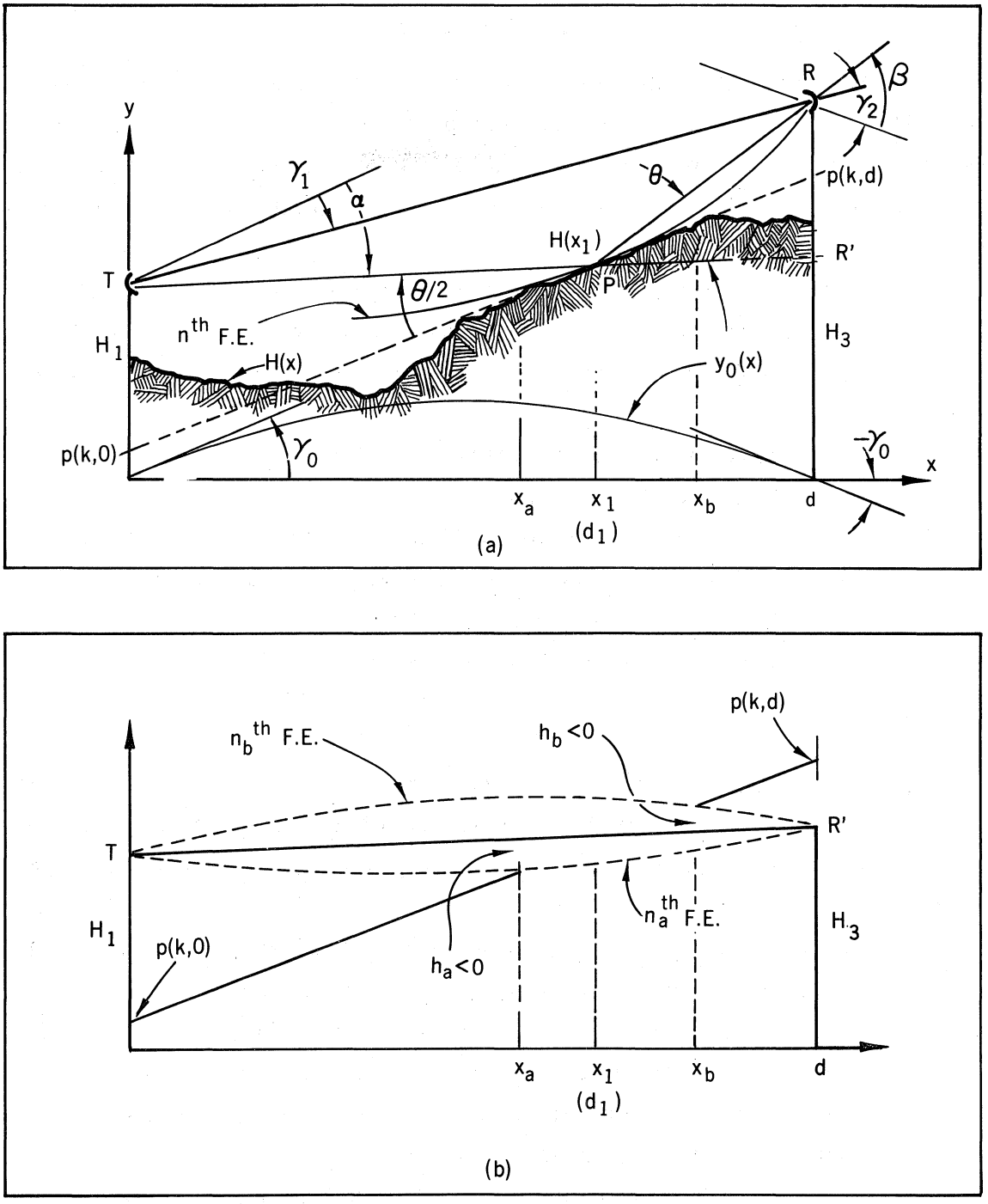

Figure 6. An example of the geometry of terrain reflection.

$\theta/2$ is the reflected path's grazing angle of incidence and reflection in milliradians;

$p(k,0)$ is the intercept in meters of the reflecting surface tangent plane at $x = 0$;

$p(k,d)$ is the intercept in meters of the tangent plane at $x = d$; and

H_3 is the elevation in meters of R', the image of the R terminal, displaced as far below the intercept $p(k,d)$ as R is above it.

The above angles are given in milliradians by expressions (11a) through (12b). Except for θ, these are all determined relative to the local horizontal plane, $\gamma_0(x)$. In Figure 6(a),

$$\gamma_0(x = 0) = \gamma_0 = \frac{d}{12.75k} \quad , \tag{15a}$$

and

$$\gamma_0(x = d) = -\gamma_0 \quad . \tag{15b}$$

3.2 Antenna Gain Factor and Phase

The partial n^{th} Fresnel ellipsoid is also illustrated in Figure 6(a). From the reflection requirement (angle of incidence equal to the angle of reflection) and the properties of an ellipsoid, the plane that is tangent to the reflecting surface at the point of reflection P is also the plane tangent to the ellipsoid (with foci at T_1 and R) through P. Therefore, the path length difference δ of Section 3 is expressible in terms of the Fresnel-ellipsoid n.

$$\delta = TPR - TR = n\lambda/2 \quad . \tag{16}$$

The relative phase angle due to this path-length difference is

$$\phi_1 = \frac{2\pi}{\lambda}\,\delta = n\pi \quad , \tag{17}$$

radians. The value of n is determined from (9), for which F_1 and $h(k,x')$ are determined from (2a) and from (8).

If we designate the antenna (vertical plane) rms power gain patterns (voltage gain patterns) as $g_1(\xi)$ and $g_2(\xi)$, where ξ is the angle off beam center, and assume that the antenna beam centers are oriented in the directions ε_1 and $-\varepsilon_2$, along the path relative to local horizontal planes, then the direct path and reflected path rms antenna power-gain factors (voltage-gain factors) are respectively

$$g = g_1(\varepsilon_1 - \gamma_1)\, g_2(\gamma_2 - \varepsilon_2) \tag{18a}$$

and

$$g_1 = g_1(\varepsilon_1 - \alpha)\, g_2(\beta - \varepsilon_2) \quad , \tag{18b}$$

where there is only i = 1 reflected path.

3.3 The Reflecting Point

Location of the reflecting point is the fundamental problem of reflection theory. In Figure 6, where these angles of grazing incidence and reflection must be equal (both equal $\theta/2$),

$$\frac{H_1 - p(k,0)}{d_1} = \frac{H_2 - p(k,d)}{d - d_1} \quad . \tag{19}$$

Given the reflection plane, as in Figure 6, the solution of (19) is straightforward,

$$d_1 = \frac{d[H_1 - p(k,0)]}{H_1 + H_2 - p(k,0) - p(k,d)} \quad . \tag{20}$$

For irregular terrain, the surface can usually be approximated in a piece-wise manner by a sequence of tilted reflecting planes. For fairly smooth terrain or over water, the surface is curved so that the tangent-reflecting plane cannot be specified until d_1 is known (and vice versa). We then define the unknown tangent-plane endpoints as p(k,0) and p(k,d) and formally define the effective antenna heights as

$$h_1 = H_1 - p(k,0) \tag{21a}$$

and

$$h_2 = H_2 - p(k,d) \quad . \tag{21b}$$

Let us introduce the notation (Norton et al., 1965)

$$A = \left| \frac{h_1 - h_2}{h_1 + h_2} \right| \quad , \tag{22a}$$

$$B = \frac{d_1 - d_2}{d_1 + d_2} \quad , \tag{22b}$$

$$d = d_1 + d_2 \quad , \tag{22c}$$

and

$$C = \frac{d^2}{25.5(h_1 + h_2)} \quad , \tag{22d}$$

where

$$A = B \left[1 + \frac{C}{k} (1 - B^2)\right] \quad . \tag{22e}$$

Again, the elevations are in meters, the distances are in kilometers, and k is the effective Earth-radius factor. For a given situation, A and C are determined from (22a) and (22d). The corresponding estimate of B, indicated as B_{eo}, is determined (for a given effective Earth factor k) from the nomograph of Figure 7. This B_{eo} is substituted into

$$B_{e1} = \frac{2B_{eo}^3 - Ak/C}{3B_{eo}^2 - 1 - k/C} \quad . \tag{22f}$$

Since (22f) is a standard Newton's method iteration procedure, presumably any B_{eo} between 0 and 1 could be used as a starting point. Thus, the need to include Figure 7 in a computer program is avoided, although the number of iterations required might be increased. In this way, B may be determined iteratively to the desired accuracy. Then for the final B value,

$$d_1 = \frac{d}{2} (1 + B) \tag{22g}$$

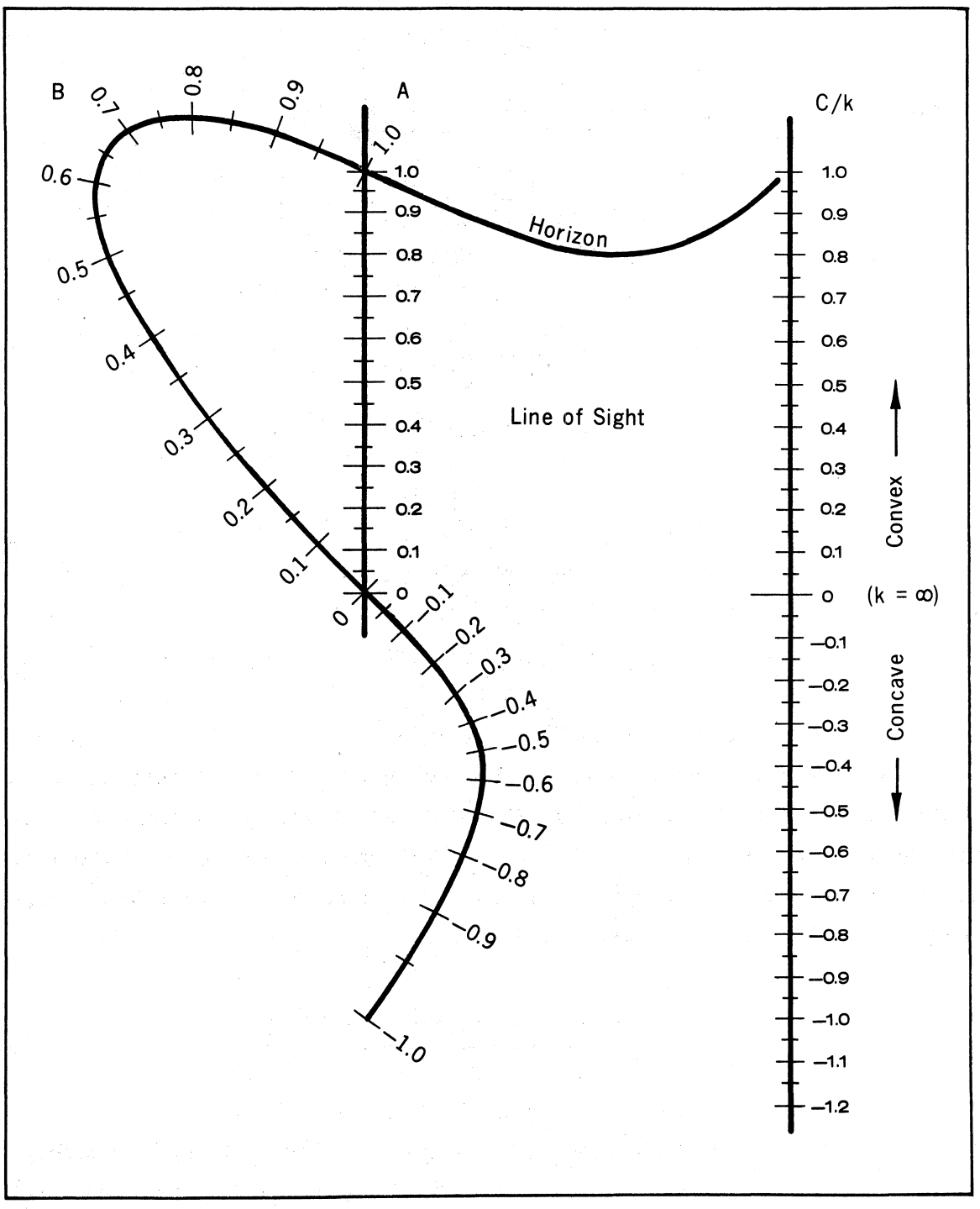

Figure 7. A nomogram relating A, B, and C/k in (22a) through (22e) (Norton et al., 1965).

and

$$d_2 = \frac{d}{2}(1 - B) \quad . \tag{22h}$$

Once the value of d_1 has been determined from (22f), (22b), and (22c), the value of the other geometrical parameters can be determined from (4a), (4b), (8), and (11a) through (16). One may then determine the antenna gain factors from (18a) and (18b) and the phase delay from (17). See the examples of Section 3.6.

3.4 The Effective Reflection Coefficients

In general, the effective reflection coefficient R is actually a composite of a number of factors:

- (o) R_+, R_- the infinite-plane reflection coefficients, also known as Fresnel reflection coefficients defined in Section 3.4.1 below;
- (o) f_v the modification factor for the finite extent of the reflecting surface;
- (o) D the divergence factor for curved surfaces; and
- (o) exp(-q) the Beckmann reflection coefficient for rough surfaces (Beckmann and Spizzichino, 1963).

3.4.1 Smooth Surfaces

The infinite plane is the simplest of the smooth surfaces. For incidence upon an infinite plane, the reflection coefficient (the ratio of the reflected field strength to the incident field strength) is known as the Fresnel coefficient

$$R_+ = \frac{\frac{\mu_o}{\mu_s} m^2 S - \sqrt{m^2 - C^2}}{\frac{\mu_o}{\mu_s} m^2 S + \sqrt{m^2 - C^2}} \quad , \quad R_- = \frac{\frac{\mu_o}{\mu_s}\sqrt{m^2 - C^2} - S}{\frac{\mu_o}{\mu_s}\sqrt{m^2 - C^2} + S} \quad . \tag{23}$$

Here, the subscripts (+ or -) refer to the polarization (vertical or horizontal) of the incident field. The $C = \cos\psi$ and $S = \sin\psi$, where ψ is the grazing angle of incidence and reflection; $\psi = \theta/2$ in Figure 6(a). The m in (23) is the refractive index of the plane surface material (relative to that of the atmosphere above the plane)

$$m = \sqrt{\frac{\mu_s}{\mu_o}} \cdot \sqrt{\frac{\varepsilon_s - j\sigma/\omega}{\varepsilon_o}} \quad . \tag{24}$$

The subscripts o and s identify the parameters for, respectively, the atmosphere and the surface. The μ is the permeability, ε is the permittivity or dielectric constant, σ is the conductivity of the surface, and $\omega = 2\pi f$, where f is the frequency.

Values of ε and σ are given in Recommendation AD/5 (CCIR, 1986b) for various types of terrain and as a function of frequency.

The R_+ and R_- values given by (23) have both magnitude and phase. At $\psi = 90°$, both expressions must become equal, since the horizontal and vertical fields are then both tangential to the surface. For application to terrain above 30 MHz, both R_+ and R_- are generally close to 1.0, and the complete reflection coefficient is more commonly determined by the other factors (D, f_v, etc.) than by R_+ or R_-.

When the smooth surface is nonplanar, the effect upon the reflection coefficient is contained in a divergence factor for convex surfaces or a convergence factor for concave surfaces. Either is given by (Norton and Omberg, 1947)

$$D = \left[1 + \frac{5d_1(d - d_1)(10)^{-3}}{16\ K\ d\ \tan\psi}\right]^{-1/2} \quad . \tag{25a}$$

Here the distances d_1 and d are in kilometers. The K is proportional to the product of the effective Earth-radius-factor k and the relative radius of curvature, r/6375, of the surface (r in kilometers) in the plane of propagation; i.e.,

$$K = kr/6375 \quad . \tag{25b}$$

If the curved surface (on a profile plotted for an effective k value) departs from the tangent an amount Δh (in meters) at a distance Δx (in kilometers) from the point of tangency, then

$$K = (\Delta x)^2/12.75\ \Delta h \quad . \tag{25c}$$

For $K > 0$, the $D < 1.0$, and for $K < 0$, the $D > 1.0$. In this latter case (concave surface), the D exceeds unity and is a convergence or focusing factor.

3.4.2 Finite Extent

In general, the reflecting portions of terrain are of limited extent. This limitation can introduce a reflection factor, f_v, that may vary between zero and about 1.2 (Norton and Omberg, 1947). The situation may be illustrated by Figure 6. There the direct propagation trajectory is between H_1 and H_2, and the reflected wave trajectory is via P or $H(x_1)$ at $x = x_1$. The reflecting surface is assumed to coincide with the indicated surface from p(k,0) to P and p(k,d), but is within LOS of <u>both</u> terminals only for the limited extent of $x_a \leq x \leq x_b$. The right-hand terminal at H_2 has an image at H_3. Note that (21b) yields

$$H_2 = p(k,d) + h_2 \quad , \tag{26a}$$

so that the image is at

$$H_3 = H_2 - 2h_2 = 2p(k,d) - H_2 = p(k,d) - h_2 \quad . \tag{26b}$$

The equivalent reflection path from H_1 to $H(x_1)$ to H_3 provides a field equivalent to that which could be transmitted from H_1 to H_3 through an aperture (Dougherty, 1969a). This aperture would extend from $x = x_a$ to $x = x_b$ in an otherwise opaque surface through p(k,0) and p(k,d), as shown in Figure 6(b). If this aperture were infinite, its transmittance would be $DR_\pm$ given by (25) and (23). Since the aperture is finite, its transmittance is modified by a factor f_v to become $f_v DR_\pm$. Thus our reflection coefficient for a smooth surface of finite extent is given by $f_v DR_\pm$.

This equivalent aperture function or finite-extent factor f_v may be evaluated by means of the dimensionless parameter

$$v = 0.00258\, h \sqrt{\frac{df}{x(d - x)}} \quad . \tag{27a}$$

Here, h is a negative obstacle height from the equivalent path (TR' in Figure 6) to the aperature edges, in this case h_a or h_b, in meters (see also the example in Section 3.6). The $x = x_a$ or x_b and d are in kilometers, and the transmission frequency is in megahertz. This parameter may also be written as

$$v = \sqrt{2n} \quad , \tag{27b}$$

where n is the Fresnel-zone number such as in (5).

From (27a), we can determine values of v_a and v_b for the obstacle heights h_a and h_b at $x = x_a$ and $x = x_b$. For the reflection angle $\theta/2$ given by the expressions (11a) through (12b), these obstacle heights are

$$h_a = \frac{\theta x_a}{2} - [H_1 - p(k_1,0)] = -\left|\frac{\theta}{2}\right|(d_1 - x_a) \tag{27c}$$

and

$$h_b = \frac{\theta x_b}{2} - [H_1 - p(k_1,0)] = -\left|\frac{\theta}{2}\right|(x_b - d_1) \quad . \tag{27d}$$

For each of $v_a = v(h_a)$ and $v_b = v(h_b)$, we determine from Figure 8 the Fresnel-Kirchhoff function values $F(v_a)$ and $F(v_b)$. The finite-extent factor is determined from their antilogs $f(v_a)$ and $f(v_b)$. That is

$$f_v\, e^{-j\phi(v)} = f(v_a)\, e^{-j\phi(v_a)} + f(v_b)\, e^{-j\phi(v_b)} - 1 \quad , \tag{28a}$$

when

$$F(v_a) = 20 \log|f(v_a)| \quad , \tag{28b}$$

etc. The phases $\phi(v_a)$ and $\phi(v_b)$ are determined from Figure 8.

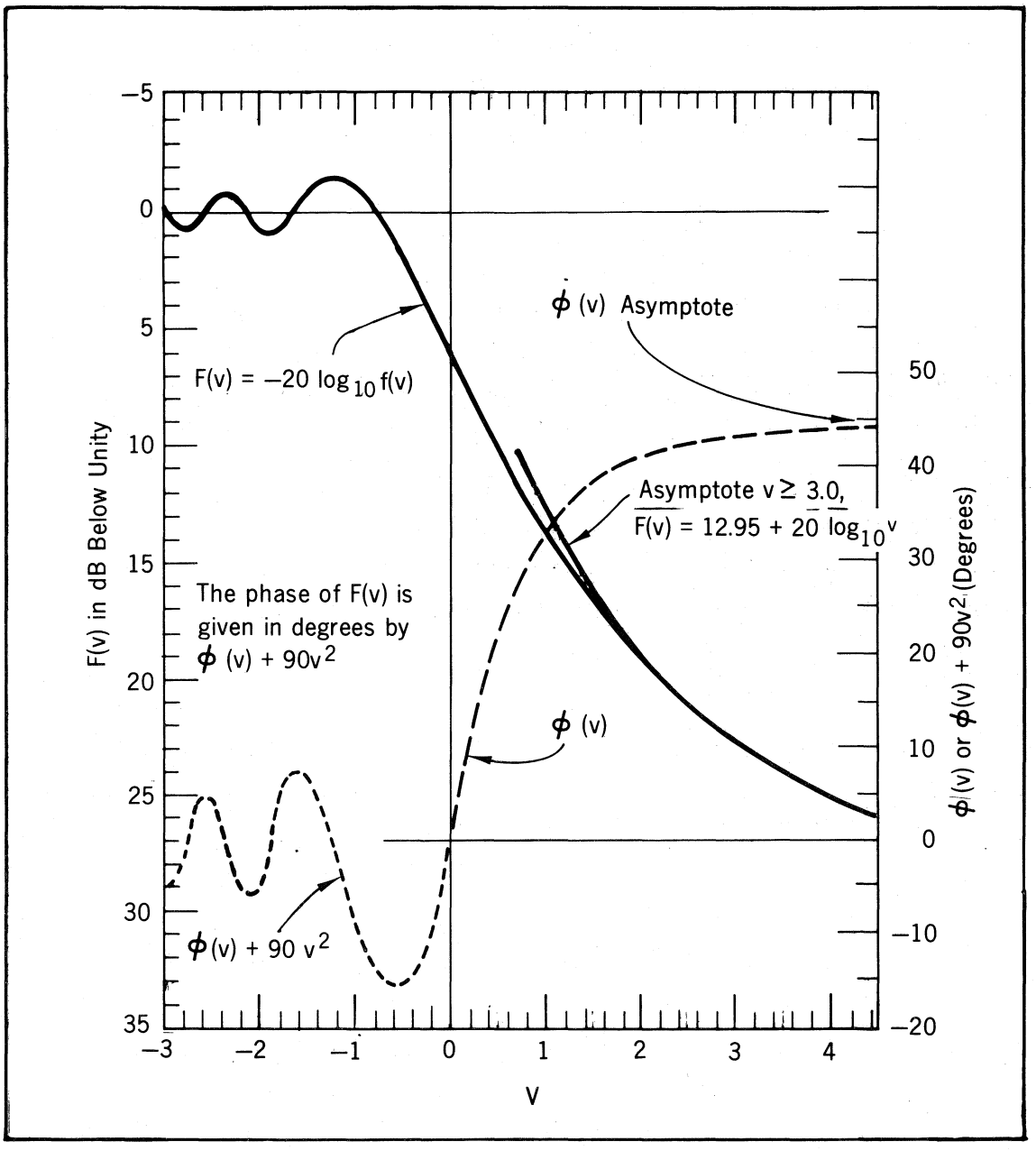

Figure 8. Components of the Fresnel-Kirchoff function (Dougherty, 1968).

Note from (27a) that v increases with frequency. The effect of increasing frequency is an increase in the effective extent of a given reflecting surface; i.e., increase the number of Fresnel zones within the terrain "aperture."

3.4.3 Rough Surfaces

Although terrain surfaces, land or sea, often crudely resemble smooth surfaces, there is almost always a surface roughness. As a result, we can often describe the terrain by a mean (smooth) surface with superimposed, randomly distributed departures from that mean surface. For reflection purposes, we can consider the smooth surface to provide specular reflection (angle of incidence equal to angle of reflection); the surface roughness provides the randomly distributed (nonspecular) reflection. This nonspecular component may be considered as the sum of specular reflections from randomly distributed facets of the terrain.

One measure of the terrain roughness is the standard deviation of the randomly distributed departures. Then a useful parameter for evaluating the effect of this roughness upon reflection is given by (Beckmann and Spizzichino, 1963)

$$q = \left[4\pi \frac{\sigma}{\lambda} \sin\psi\right]^2 \quad . \tag{29}$$

Here, λ is the transmission wavelength in meters, σ is the standard deviation* of the terrain departures in meters, and ψ, in radians, is the reflection angle or $\theta/2$ as indicated in Figure 6(a).

Because of this roughness, the specular reflection coefficient is reduced by the factor

$$R(q) = e^{-q/2} \quad . \tag{30}$$

---

*Note that henceforth σ will be used to represent terrain departure standard deviation rather than surface conductivity as in (24).

The Rayleigh-distributed nonspecular components would have a median level of approximately 1 - R(q). Note in (29) that decreasing wavelengths or increasing frequency increases the value of q and reduces the specular reflection coefficient. Of course, small values of ψ tend to offset increases in σ/λ. As σ/λ becomes very large (with increasing frequency), this tends to be offset by the fact that portions of the terrain irregularities tend to become more efficient reflection surfaces because of the effects described in Section 3.4.2. For example, the irregular sea surface can still specularly reflect sunlight because the irregularities contain surface facets that are extensive in terms of Fresnel zones and visible wavelengths.

3.5 Reflected Signal Distributions

From the preceding discussion, one can conclude that the field reflected from the terrain may be represented by a specular component given by (23), (26), (28), and (30) as

$$R = R(q)\, f_V DR_{\pm} \quad , \tag{31}$$

relative to the incident field. In addition to this specularly reflected component, there will be a nonspecular component. If the terrain irregularities that provide the terrain roughness are random, this nonspecular reflected component is Rayleigh distributed. If there is an asymmetry to the roughness (such as for the alignment of waves that can occur with water), the field may have a Hoyt (asymmetrical Rayleigh) distribution (Beckmann and Spizzichino, 1963). For q given by (29) as approximately unity or less, the reflected field will be described by a constant (specular component) plus a Rayleigh (nonspecular component) distribution. This "constant-plus-a-Rayleigh" total reflected field must then be combined with the direct field component to determine the total received field (Dougherty, 1968). Of course, the direct field component and a Rayleigh total reflected component can also describe a "constant-plus-Rayleigh" (Nakagami-Rice) distributed field.

3.6 Examples

Consider the situation represented by Figure 5 and the parameter values:

H_1	= 35 m	$p(k,0)$	= 8.5 m	k	= 4/3
H_2	= 60 m	$p(k,d)$	= 47.5 m	12.75 k	= 17
d	= 25 km	x_a	= 14.4 km	σ	= 0.1 m
d_1	= 17 km	x_b	= 18.0 km	ε_1	= γ_0
$y(P)$	= 35 m	f	= 4 GHz	ε_2	= $\pi - \gamma_0$
$H(P)$	= 27 m	$D_1=D_2$	= 2 m	λ	= 0.075 m.

Here the D_1 and D_2 are the diameters of two parabolic antennas at H_1 and H_2. At the f = 4 GHz, the half-power beamwidth is $\Omega \approx 2.6°$ or 45.4 mrad, and the antennas are directed along the local horizontal plane.

From (1f), (11b), and (11c), for $x_1 = x_2 = d_1$, γ_o = 25/17 = 1.47 mrad,

$$\alpha = \frac{27 - 35}{17} - \frac{17}{17} = -1.47 \text{ mrad} \quad ;$$

$$-\beta = \frac{27 - 60}{8} - \frac{8}{17} = -4.60 \text{ mrad} \quad .$$

From (12a) and (12b),

$$\gamma_1 = \frac{60 - 35}{25} - \frac{25}{17} = -0.47 \text{ mrad} \quad ;$$

$$\gamma_2 = -0.47 + \frac{50}{17} = 2.47 \text{ mrad} \quad .$$

Since the reference for these angles is the local horizontal, these angles, γ_1 and $\pi - \gamma_2$, are also the directional angles relative to beam center. All are small relative to the beamwidth (~0.1 Ω). The effective antenna gain for each path, given by (18a) and (18b), will be less than 0.2 dB below the combined mainbeam power gains of 2(36) = 72 dBi or voltage gains of $g=g_1$ 4000.

Checking the reflection point location from (19),

$$\frac{35 - 8.5}{17} = \frac{60 - 47.5}{8} = 1.5607 \pm 0.0019 \quad ;$$

i.e., they agree to within 0.2 percent.

From Section 2.6.2, n = 0.707, so that (17) yields

$$\phi = 0.707\pi = 2.22 \text{ rad} = 127 \text{ deg} \quad .$$

To evaluate the divergence factor at P in Figure 5, we note that at $x = x_a = 14.4$ km the curved surface is 1.0 m below the plane tangent at $x = 17$ km. From (25c),

$$K = \frac{(17 - 14.4)^2}{12.75(1)} = 0.53 \quad .$$

From (11a) and (25a),

$$\theta = -1.47 - 4.60 + 50/17 = -3.13 \text{ mrad}$$

$$\psi = |\theta/2| = 1.56 \text{ mrad}, \; 10^3 \tan 10^{-3} \psi = 1.56$$

$$D = \left[1 + \frac{5(17)8}{16(0.53)25(1.56)}\right]^{-1/2} = 0.57 \quad .$$

To evaluate the limited extent of the curved reflecting surface for $x_a \leq x \leq x_b$, we note from (26a) and (26b) that

$$h_2 = 60 - 47.5 = 12.5 \text{ m}$$
$$H_3 = 60 - 2(12.5) = 35 \text{ m}.$$

The obstacle heights for the aperture edges defined by the plane aperture, illustrated by Figure 6(b), are given by (27c) and (27d). However, for the obstacle heights for the aperture edges defined by the terrain, we must also include the height intervals between the plane and the terrain. That is, at $x_a = 14.4$ km, we must add the 1.0 m to the computation of (27c) to determine

h_a. Similarly, at x = 18 km, we must add the 0.15 m to the computation of (27d) to determine h_b. Both obstacle heights are negative. This is because the reflection plane aperature can be thought of as essentially an "opening" in the terrain, in which case the "heights" on either side are negative obstacle heights (aperature edges) with respect to, say, the path TPR' in Figure 6a. This is also why a negative sign is placed in front of the following calculations for h_a and h_b

$$h_a = -\{1.0 + [1.56(14.4) - (35 - 8.5)]\} = -5.04 \text{ m}$$

and

$$h_b = -\{0.15 + [1.56(18) - 26.5]\} = -1.73 \text{ m} \quad .$$

From (27a)

$$v_a = 0.00258(-5.04) \quad \frac{25(4000)}{14.4(10.6)} = -0.333$$

and

$$v_b = 0.00258(-1.73) \quad \frac{25(4000)}{18(7)} = -0.126 \quad .$$

From Figure 8, $F(f_a)$ and $F(v_b)$ are respectively 2.9 and 7.0 dB, with phase angles of -14.5 deg and -8.0 deg,

$$f(-0.333) = 0.72\, e^{+j14.5}$$

and

$$f(-0.126) = 0.54\, e^{+j8.0} \quad .$$

From (28),

$$\begin{aligned} f_v &= 0.72 \cos 14.5 + 0.54 \cos 8.0 - 1 + j[0.72 \sin 14.5 + 0.54 \sin 8.0] \\ &= 0.232 + j0.255 \\ &= 0.345 e^{+j(47.7)} \quad . \end{aligned}$$

The roughness factor, i.e., the Beckmann and Spizzichino (1963) coefficient, is determined from (29) and (30)

$$q = \left[4\pi \frac{0.1}{0.075} 0.00156\right]^2$$
$$= 0.00068 .$$

$$R(q) = e^{-0.5(0.00068)} \simeq 1.0 .$$

The total reflection coefficient (31) is therefore

$$R = (1.0)\ (0.345)\ (0.57)\ R_{\pm} = 0.197R_{\pm} .$$

Notice that at this extremely small reflection angle (1.56 mrad, or less than 0.1°) the divergence factor is one of the dominant factors reducing R. As larger reflection angles are considered, the role of the divergence factor is reduced and the roughness factor comes to play a more significant role. To illustrate this, we note that if $|\theta/2|$ were increased by a factor of 50 to a value of 78 mrad or 4.4 deg and if all other factors were unchanged, the divergence factor D would increase from 0.57 to 0.98 while the roughness factor R(q) decreased from 1.0 to 0.438.

4. DIFFRACTION

When the Fresnel-zone clearance of an LOS path becomes less than $n_c = 0.3$ or when a transition from LOS path to transhorizon path occurs, the field may be determined by the diffraction formulas summarized in this section.

One exception is the situation for which the antennas are within a few wavelengths of the surface. The resultant fields then tend to be sensitive to the surface electrical constants and are most readily determined from the plotted CCIR groundwave curves (CCIR, 1986c, 1986d).

A second exception is encountered on transhorizon paths for large diffraction angles. Then the diffracted field is sufficiently weak so that the troposcatter mode of propagation provides the dominant field (CCIR, 1986a).

4.1 Isolated Terrain Features

If the terminal antennas are sufficiently remote from the surface of a terrain feature that partially or fully obstructs a wave propagation path, such as in Figures 2(b), 2(c), and 9, the field E may be expressed relative to the free-space field E_o by the attenuation expression in decibels (CCIR, 1986c)

$$20 \log_{10} \frac{E_o}{E} = A = F(v) + G(\rho) + H(\chi) \quad . \tag{32}$$

The Fresnel-Kirchhoff function F(v) is given in Figure 8 in terms of the parameter v. The v is given by (27a), but a more general expression (CCIR, 1986c) is

$$v = 5.166 \sin\left(\frac{\theta}{2000}\right) \left[\frac{\left(d_a + \frac{R\theta}{2000}\right)\left(d_b + \frac{R\theta}{2000}\right) f}{d}\right]^{1/2} , \tag{33a}$$

where R is the effective radius of curvature (in kilometers) of the obstacle in the plane defined by T_1PT_2 in Figure 9. If the actual obstacle radius is r, the effective radius is given by (25b), (25c), and R = 6375 K. The distances from each terminal to its point of tangency on the obstacle, d_a and d_b, are in kilometers (see Figure 9). The $R\theta/1000$, for θ in milliradians, is the distance (in kilometers) on the obstacle surface between the tangency points. The d is the total path length in kilometers, and f is the transmission frequency in megahertz. Alternate forms for (33a) are available utilizing θ in milliradians

$$\theta \quad 10^3 \sin 10^{-3}\theta = \frac{hd}{(d_a + R\theta/2000)(d_b + R\theta/2000)} \tag{33b}$$

or

$$\theta = \theta_1 + \theta_2 \quad , \tag{33c}$$

where

$$\theta_1 = \alpha - \gamma_1, \quad \theta_2 = -[\beta - \gamma_2] \quad . \tag{33d}$$

The α, β, γ_1, and γ_2 are given by (11a) through (12b). Note that v has the sign of θ or h, which are defined as negative when the obstacle peak (at P) lies below the LOS path T_1T_2. See Figure 9.

The $G(\rho)$ in (32) is the loss in decibels due to incidence upon the curved obstacle surface and is determined from (CCIR, 1986c)

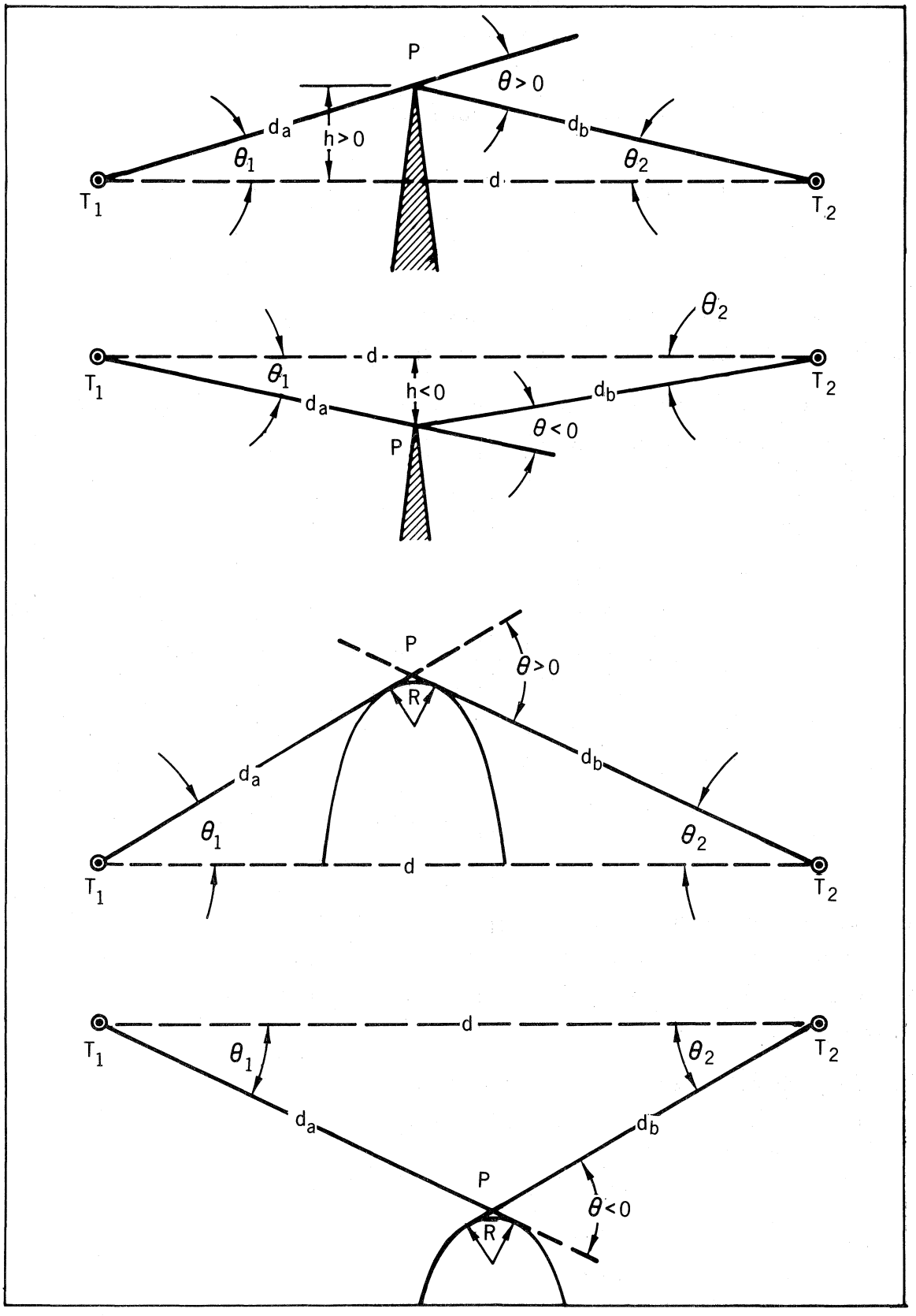

Figure 9. Diffraction path geometry for isolated terrain features.

$$G(\rho) = 7.192\rho - 2.018\rho^2 + 3.63\rho^3 - 0.754\rho^4 \quad , \tag{34a}$$

where the dimensionless normalized radius ρ is given by

$$\rho^2 = \frac{d_a + d_b}{10\, d_a d_b} \Big/ \left[\left(\frac{\pi R}{\lambda} \right)^{1/3} \frac{1}{R} \right] = \frac{0.457}{(Rf)^{1/3}} \frac{R(d_a + d_b)}{d_a d_b} \quad . \tag{34b}$$

The transmission wavelength λ is in meters and is approximately 300/f for f in megahertz. The R, d_a, and d_b are in kilometers.

The $H(\chi)$ in (32) is the decibel loss for propagation along the surface between the horizons and is given by (CCIR, 1986c)

$$H(\chi) = \begin{cases} 1.03 \dfrac{G(\rho)}{\rho} \chi, \text{ for } -0.9708\ \rho \le \chi \le 0 \\ 12\chi, \text{ for } 0 \le \chi \le 4 \\ 17.1\chi - 6.2 - 20\log\chi, \text{ for } \chi > 4 \end{cases} \quad . \tag{35a}$$

where, for θ in mrad, R in km, and λ in m or f in MHz,

$$\chi = \left(\frac{\pi R}{\lambda} \right)^{1/3} \theta(10)^{-2} = 0.00219\ \theta(Rf)^{1/3} \quad . \tag{35b}$$

As R approaches zero, ρ and χ approach zero and (32) reduces to its first term, F(v). For $\theta = 0$, $\chi = 0$, and $H(\chi) = 0$; further, $v = 0$, $F(v) = 6$ dB, and (32) then gives the loss for grazing incidence upon the obstacle or rounded knife-edge.

The foregoing expressions assume that all of the distances (in kilometers) are large relative to the transmission wavelength (in meters); specifically,

$$\left[\left(\frac{\pi R}{\lambda} \right)^{1/3} / R \right]^2 d_a d_b \ge 10^{-3} \quad . \tag{36}$$

These diffraction expressions are usually applicable for either polarization,

for the ground constants normally encountered for terrain, and for frequencies above about 10 MHz. An exception is for vertical polarization at frequencies below 1 GHz, when the path is over sea water. For over-sea paths with vertical polarization at frequencies below 1 GHz, see CCIR (1986d). It is important to note, however, that in the now extensively used region above 1 GHz, even this exception disappears.

4.2 Irregular Terrain

Commonly on transhorizon paths, the horizons of both terminals are determined by different terrain features. This is illustrated by Figure 10. The formulas for the isolated terrain feature are readily extended to provide an estimate of the total diffraction loss relative to free space:

$$20 \log \frac{E_o}{E} = F(v_o) + \frac{1}{2} G(\rho_1) + \frac{1}{2} G(\rho_2) + H(\chi_o) \quad . \tag{37a}$$

Here we have appended subscripts to the parameters v, ρ, and χ to identify their association with the specific radii

$$R_o = 10^3 \, d_s/\theta \quad , \tag{37b}$$

$$R_i = 6375 \, K_i, \; i = 1,2 \quad . \tag{37c}$$

Here, the radii are in kilometers when the distance between the horizons is d_o in kilometers and the diffraction angle is θ in milliradians. The K_i are the effective-Earth-radius factor appropriate to each end of the path, given by (25b) or (25c). The applications of (37a) through (37c) are illustrated by the examples of Section 4.4.

Recently, other methods have been developed and extended for analysis of irregular terrain (e.g., Vogler, 1982), although these methods are still relatively too sophisticated for personal computer adaptation.

4.3 Effect of Vegetation

The presence of vegetation (trees, bushes) along the propagation path introduces an additional attenuation. This is illustrated by Figure 11.

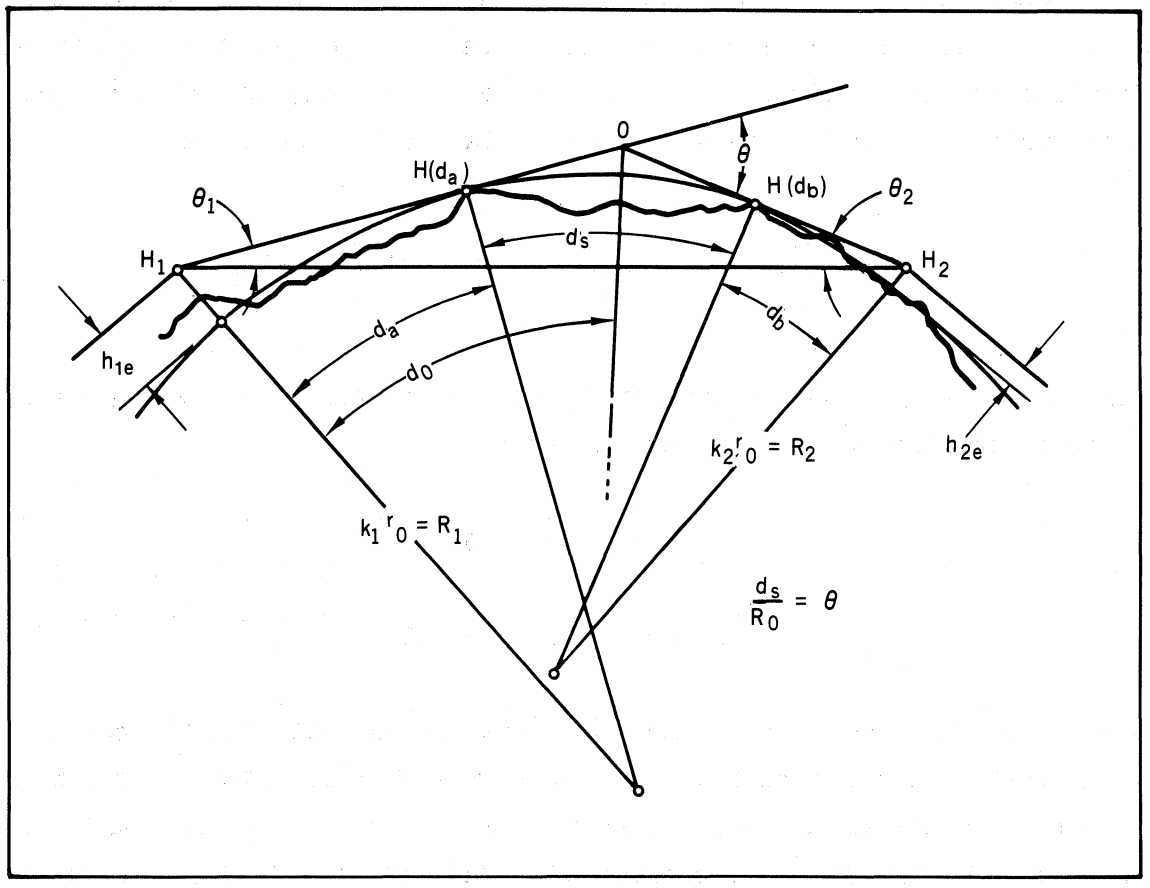

Figure 10. Geometry for diffraction over irregular terrain.

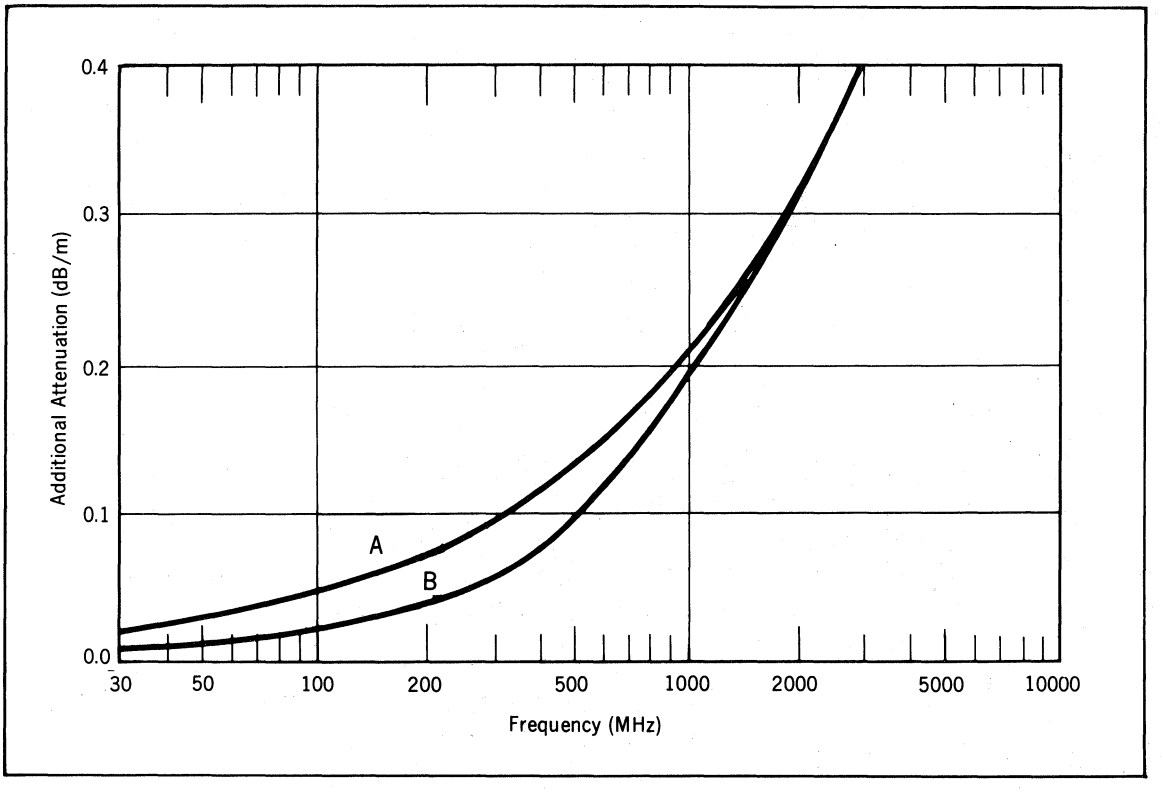

Figure 11. Additional attenuation through wooded terrain. Curve A is for transmitted vertical polarization and curve B is for transmitted horizontal polarization (CCIR, 1986e).

Above about 1.0 GHz and for either polarization, the vegetation becomes increasingly opaque to radio waves. When the system terminals are positioned above or outside wooded regions, a common approach is to simply add to the terrain elevation an additional amount equal to the median height of the trees (CCIR, 1986e).

4.4 Examples

The preceding diffraction formulas will be illustrated by two situations. In the first situation, the transhorizon path will have the terminal horizons located on a common isolated terrain feature. In the second situation, the transhorizon path will have the terminals horizons on separate terrain features.

4.4.1 An Isolated Terrain Feature

Consider the situation of the lower-most diagram of Figure 9, which depicts an isolated obstacle. On a larger, scaled, k = 4/3 plot of a similar terrain profile, the radius of curvature is R = 1360 km for an obstacle at x_o = 17 km from the left-hand terminal. Further examination of the profile determines that the straight-line wave trajectories from each terminal ($H_1 = H_2$ = 60 m, d = 25 km) to horizons on the terrain intersect at y = 54 m and x_o = 17 km from the left-hand terminal. A straight-line trajectory from the left-hand terminal is tangent to the near-obstructing terrain feature at y(x = 18) = 51.53 m. Similarly, a straight-line trajectory from the right-hand terminal is tangent at y(x = 16) = 51 m.

From (1i),

$$H(18) = H_o(k = 4/3,\ x = 18) = 51.53 - \frac{18(7)}{17} = 44.12 \text{ m}$$

and

$$H(16) = H_o(k = 4/3,\ x = 16) = 51.0 - \frac{16(9)}{17} = 42.53 \text{ m} \quad .$$

From (25b) and (25c),

$$\Delta h = \frac{(1.0)^2(6375)}{12.75(4/3)1360} = 0.276 \text{ m} \quad .$$

Therefore, at x = 17 km, a distance Δx = 1 km from either horizon, the terrain is

$$y(17) = 54 - 0.28 = 53.72 \text{ m} \quad , \quad H(17) = 53.72 - \frac{17(8)}{17} = 45.72 \text{ m} \quad .$$

From (11a) through (12b) and (33c) through (33d),

$$\alpha = \frac{44.12 - 60}{18} - \frac{18}{17} = -1.9410, \qquad -\beta = \frac{42.53 - 60}{9} - \frac{9}{17} = -2.4705$$

$$\gamma_1 = \frac{60 - 60}{25} - \frac{25}{17} = -1.4706, \qquad \gamma_2 = -1.4706 + \frac{50}{17} = +1.4706$$

$$\theta_1 = -1.9410 + 1.4706 = -0.4704, \qquad \theta_2 = -2.4705 + 1.4706 = -0.9999$$

$$\theta = -0.4704 - 0.9999 = -1.4703, \quad \frac{R\theta}{2000} = -(0.73513)(1.360) \quad -1.0 \quad .$$

From (33a) at f = 4 GHz,

$$v = 5.166(-0.735)10^{-3}\left[\frac{(18 - 1)(9 - 1)\ 4000}{25}\right]^{1/2}$$

$$= -0.3798\left[\frac{17(8)}{25}\ 0.4\right]^{1/2} = -0.56 \quad .$$

From Figure 8, F(-0.56) = 1.3 dB. From (34a) and (34b),

$$\rho^2 = \frac{18 + 9}{18(10)9} \Big/ \left[\left(\frac{\pi 1.36}{300}\ 4(10)^6\right)^{1/3}\ \frac{1}{1360}\right] \quad ,$$

$$\rho \simeq 0.77$$

$$G(\rho) = 7.192(0.77) - 2.018(0.77)^2 + 3.63(0.77)^3 - 0.754(0.77)^4$$

$$= 5.73 \text{ dB} \quad .$$

From (35b),

$$\chi = -\left[\frac{\pi(1.36)4(10)^6}{300}\right]^{1/3} 1.4703(10)^{-2}$$

$$= -3.847(1.4703)10^{-1} = -0.566 \quad .$$

From (35a),

$$H(\chi) = -0.566(1.03)\frac{5.73}{0.77} = -4.3 \text{ dB} \quad .$$

From (32),

$$A = 1.3 + 5.7 - 4.3 = 2.7 \text{ dB} \quad .$$

Examination of the terrain profile considered above indicates that if the left-hand terminal were lowered to H_1 = 35 m and the right-hand terminal were lowered to H_2 = 48.24, the situation would be similar to the second lower-most diagram of Figure 9. The $y(x = 16) = 51$ m would become the horizon of the left-hand terminal (i.e., $d_a = 16$ km). The $y(x = 18) = 51.53$ would become the horizon of the right-hand terminal (i.e., $d - d_b = 7$). The θ_1, θ_2, θ, v, and χ values would then simply change sign. Thus,

$$v = 0.56 \text{ so that } F(v) = 10.9 \text{ dB} \quad ,$$
$$\chi = 0.566 \text{ so that } H(0.566) = 0.566(12) = 6.8 \text{ dB} \quad ,$$

but ρ^2 and $G(\rho)$ would be the same. Therefore,

$$A = 10.9 + 5.7 + 6.8 = 23.4 \text{ dB} \quad .$$

4.4.2 Irregular Terrain

Consider the situation of Figure 5. Note that the propagation path would become transhorizon for $k = 4/3$ if the terminals T_1 and T_2 were lowered to T_1' at $H_1 = 30$ m and to T_2' at $H_2 = 38.3$ m. The associated path parameters depicted in Figure 10 can be applied to Figure 5 to determine that

d_a	= 8 km	d_b	= 21 km	d	= 25 km
$H(d_a)$	= 26 m	$H(d_b)$	= 33.4 m	d_s	= 13 km
$y(d_a)$	= 34 m	$y(d_b)$	= 38.3 m	d_o	= 16.6 km
n	= 0.019	H(0)	= 25 m	H(d)	= 35 m.

From (25c) and (37c),

$$K_1 = \frac{(8)^2}{12.75(30 - 25)} = 1.004$$

and

$$R_1 = 6375(1.004) = 6400 \text{ km} \quad .$$

Similarly,

$$K_2 = \frac{(4)^2}{12.75(38.3 - 35)} = 0.3802$$

and

$$R_1 = 6375(0.3802) = 2424 \text{ km} \quad .$$

From (34b)

$$\rho_1^2 = \frac{0.457(6400)(8 + 4)}{4(8)[(6400)4000]^{1/3}}$$

$$= 0.171 \left(\frac{6400}{294.72}\right) = 3.71$$

$$\rho_1 = 1.93$$

$$\rho_2^2 = 0.171(2424) \; / \; [(2424)4000]^{1/3}$$

$$= 0.171 \left(\frac{2424}{213.24}\right) = 1.94$$

$$\rho_2 = 1.39 \quad .$$

Then, from (34a),

$$\frac{1}{2} G(\rho_1) + \frac{1}{2} G(\rho_2) \approx 10.99 + 6.51 = 17.5 \text{ dB} \quad .$$

From (27b), $v_o = \sqrt{2n} = 0.19$. From Figure 8, $F(v_o) = 7.1$ dB. From (37b),

$$R_o = 13(10)^3/0.5 = 26{,}000 \text{ km} \quad .$$

Note, $\theta = 0.5$ mrad is determined as before using (11b), (11c), (12a), (12b), (33d), and (33c). At $f = 4$ GHz, from (35b),

$$\chi_o = 2.19(10)^{-3}\ 0.5[26(4)]^{1/3}\ (10)^2$$
$$= 0.1095[104]^{1/3} = 0.515 \quad .$$

From (35a), $H(\chi_o) = 12(0.515) = 6.18$ dB. From (37a),

$$20 \log \frac{E_o}{E} = 7.1 + 17.5 + 6.18 \text{ dB}$$

$$= 30.78 \text{ dB} \quad .$$

5. EFFECTS OF THE TRANSVERSE PROFILE

For propagation between a transmitter and receiver, the plane of propagation is defined as that containing the Earth's center and the two terminal antenna centers of radiation. Normally, the wave trajectories between the terminals will lie in this plane. The intersection of this plane with the Earth's surface defines the great-circle path and the terrain profile.

In the preceding sections, the formulations of the terrain effects assume that the terrain profile elevations do not change normal to the plane of propagation and, therefore, the wave trajectories all lie in this plane of propagation. If, as is common, the terrain profile elevations do change, normal to the propagation path (and normal to the terrain profile), then there are correction factors required for some of the preceding formulations.

Consider, for example, the situation illustrated by the terrain point P of Figure 5. The formulas applied in Section 3.6 assume that the elevations do not change normal to the T_1PT_2 plane of Figure 5; that is, the rounded terrain profile through P was assumed to be the cross-section of a (rounded knife-edge) ridge normal to the terrain profile. However, if it were the cross-section of a rounded hill, a correction factor would be required. For the negative obstacle height depicted in Figure 5, the effective reflection coefficient in (6) would require an additional divergence factor determined from (25a) through (25c) for the transverse profile radius of curvature.

In Section 4.4.2, the situation of Figure 5 was reevaluated, with lowered antenna center-of-radiation elevations, as a transhorizon path. If the terrain of P were the cross-section of a rounded hill, a correction term of $0.5\ T_c$ in decibels would have to be added to (37a), given by (Dougherty, 1969a and 1969b)

$$T_c = -10 \log_{10} \left[1 - \frac{\left(d_a + \frac{R\theta}{2000} \right) \left(d_b + \frac{R\theta}{2000} \right)}{K_c\, d} \left(\sin \frac{\theta}{1000} \right) \right] . \qquad (38)$$

Here, the K_c is the normalized radius of curvature determined from (25b) and (25c) for the transverse profile's radius of curvature at P. The other parameters are as defined in (33a) and for the same specified units.

The lowered antenna elevations referred to above for Figure 5 provide a left-hand horizon of H = 26 m at d_a = 8 km, or $y(x = 8) = 34$ m. That terrain feature at x = 8 km in Figure 5 is peaked. If it also had a triangular transverse cross-section with an interior apex angle of $\nu\pi$, $0 < \nu < 2$, then (37a) would need an additional correctional term $0.5\ T_\Lambda$ in decibels, given by (Dougherty, 1970b)

$$T_\Lambda = 20 \log_{10}(2 - \nu) \quad . \qquad (39)$$

It should be noted that a transverse profile that provides a horizon on a propagation path's terrain profile may thereby create more than one wave trajectory. For example, energy can be diffracted around an obstacle as well

as over it. When there is more than one diffracted wave trajectory, a weighting factor is required. This weighting factor, which is detailed in Dougherty (1970a), has an asymptotic value of unity for sufficiently separated diffracting points.

6. CONCLUSIONS

This report has detailed the evaluation of the geometrical parameters for terrain along the propagation path of a proposed system. Further, it has made explicit the role of these parameters in the determination of the path losses due to the reflected and diffracted fields. It has permitted the reader to gain some familiarity with the engineering expressions and gain some experience with their application to the sort of terrain situations that may be encountered in terrestrial system design. The engineer could now use these expressions to

- (o) identify those portions of a path (LOS or transhorizon) that are likely to be significant (the horizons, the potential reflecting surfaces, etc.);
- (o) estimate the expected transmission loss for a particular proposed path geometry; and
- (o) determine the quantitative effect upon that expected transmission loss of displacing one or both terminal antennas (vertically or horizontally).

By application of the engineering techniques inherent in the above, modern system design can minimize the disadvantageous aspects of terrain because it is a largely controllable problem today. While there are many reports covering the various aspects of terrain effects (e.g., Parl and Malaga, 1984), the procedures of this report are readily expressed as computer subroutines; the process of quantifying terrain effects therefore could be programmed readily or incorporated on computer chips.

7. REFERENCES

Bean, B. R., and E. J. Dutton (1968), Radio Meteorology (Dover Publications, Inc., New York, NY), p. 14.

Beckmann, P., and A. Spizzichino (1963), The Scattering of Electromagnetic Waves from Rough Surfaces (MacMillan Co., New York, NY).

CCIR (1986a), Propagation data required for trans-horizon radio-relay systems, Report 238-3, Vol. V, CCIR XVI Plenary Assembly, Yugoslavia.

CCIR (1986b), Electrical characteristics of the surface of the earth, Recommendation 527-1, Vol. V, CCIR XVI Plenary Assembly, Yugoslavia.

CCIR (1986c), Propagation by diffraction, Report 715-1, Vol. V, CCIR XVI Plenary Assembly, Yugoslavia.

CCIR (1986d), Ground-wave propagation curves for frequencies between 10 kHz and 10 MHz, Recommendation 368-3, Vol. V, CCIR XVI Plenary Assembly, Yugoslavia.

CCIR (1986e), Influence of terrain irregularities and vegetation on tropospheric propagation, Report 236-5, Vol. V, CCIR Plenary Assembly, Yugoslavia.

Dougherty, H. T. (1968), A survey of microwave fading mechanisms, remedies and applications, ESSA Tech. Report No. ERL 69-WPL4 (NTIS Order No. COM-71-50288*).

Dougherty, H. T. (1969a), An expansion of the Helmholtz integral and its evaluation, Radio Sci. 4, No. 11, pp. 991-995, November.

Dougherty, H. T. (1969b), Radio wave propagation for irregular boundaries, Radio Sci. 4, No. 11, pp. 997-1004, November.

Dougherty, H. T. (1970a), Diffraction by irregular apertures, Radio Sci. 5, No. 1, pp. 55-60, January.

Dougherty, H. T. (1970b), The application of stationary phase to radio propagation for finite limits of integration, Radio Sci. 5, No. 1, pp. 1-6, January.

Dougherty, H. T. (1981), Electromagnetic wave trajectories at VHF and higher frequencies, NTIA Contractor Report 81-14, October (NTIS Order No. PB 82-134289*).

Millington, G. (1957), The concept of the equivalent radius of the Earth in tropospheric propagation, Marconi Rev. 20, pp. 79-93, January.

Norton, K. A., G. A. Hufford, H. T. Dougherty, and R. E. Wilkerson (1965), Diversity design for within-the-horizon radio relay systems, NBS Report 8787 (NTIS Order No. COM-73-10103*).

Norton, K. A., and A. C. Omberg (1947), The maximum range of a radar set, Proc. IRE 35, pp. 4-24, January.

---

*Address for NTIS: National Technical Information Service, P.O. Box 1553, Springfield, VA 22161.

Parl, S., and A. Malaga (1984), Theoretical analysis of microwave propagation, Rome Air Development Center Report RADC-TR-84-74 (Rome Air Development Center, Air Force Systems Command, Griffiss Air Force Base, NY 13441), April.

Rice, P. L., A. G. Longley, K. A. Norton, and A. P. Barsis (1967), Transmission loss predictions for tropospheric communications circuits, NBS Tech. Note 101, Vol. I and II, May (NTIS Order No. AD 687820 and AD 687821*).

Vogler, L. E. (1982), An attenuation function for multiple knife-edge diffraction, Radio Sci. 17, No. 6, pp. 1541-1546, November-December.

FORM **NTIA-29**
(4-80)

U.S. DEPARTMENT OF COMMERCE
NAT'L. TELECOMMUNICATIONS AND INFORMATION ADMINISTRATION

BIBLIOGRAPHIC DATA SHEET

	1. PUBLICATION NO.	2. Gov't Accession No.	3. Recipient's Accession No.
	NTIA Report 86-200		

4. TITLE AND SUBTITLE

Quantifying the Effects of Terrain for VHF and Higher Frequency Application

5. Publication Date
July 1986

6. Performing Organization Code
NTIA/ITS.S2

7. AUTHOR(S)
H. T. Dougherty and E. J. Dutton

9. Project/Task/Work Unit No.
9104519

8. PERFORMING ORGANIZATION NAME AND ADDRESS
U.S. Department of Commerce
NTIA/ITS.S2
325 Broadway
Boulder, CO 80303

10. Contract/Grant No.

11. Sponsoring Organization Name and Address
National Security Agency
9800 Savage Rd.
Ft. Meade, MD 20755

12. Type of Report and Period Covered
NTIA Report

13.

14. SUPPLEMENTARY NOTES

15. ABSTRACT *(A 200-word or less factual summary of most significant information. If document includes a significant bibliography or literature survey, mention it here.)*

This report is tutorial in presentation, with emphasis on the application of engineering formulations of the effects of terrain upon terrestrial microwave systems. Many of these formulas have been available for a decade and longer, but they have not been widely used. Although they are well based in theory and experiment, their applications had been considered too detailed and tedious until the present widespread availability of personal computers. Therefore, these formulas have been presented here in a form readily adaptable as computer programs and subprograms. The units are carefully specified for use with terrain data bases for incorporation in a system design that would permit tradeoffs between terrain geometry, hardware parameters, and system performance criteria. There are additional formulations similarly well based in theory and experiment; they are not presented here, but they are adequately referenced. The readers should consider them for an increased sophistication of their system design.

16. Key Words *(Alphabetical order, separated by semicolons)*

clearance; diffraction; Earth's surface; engineering formulation; Fresnel zones; link design; radio horizons; reflection; terrain; terrestrial-link propagation

17. AVAILABILITY STATEMENT

☒ UNLIMITED.

☐ FOR OFFICIAL DISTRIBUTION.

18. Security Class. *(This report)*
Unclassified

20. Number of pages
54

19. Security Class. *(This page)*
Unclassified

21. Price:

☆U.S. GOVERNMENT PRINTING OFFICE:1986—676-002/40026